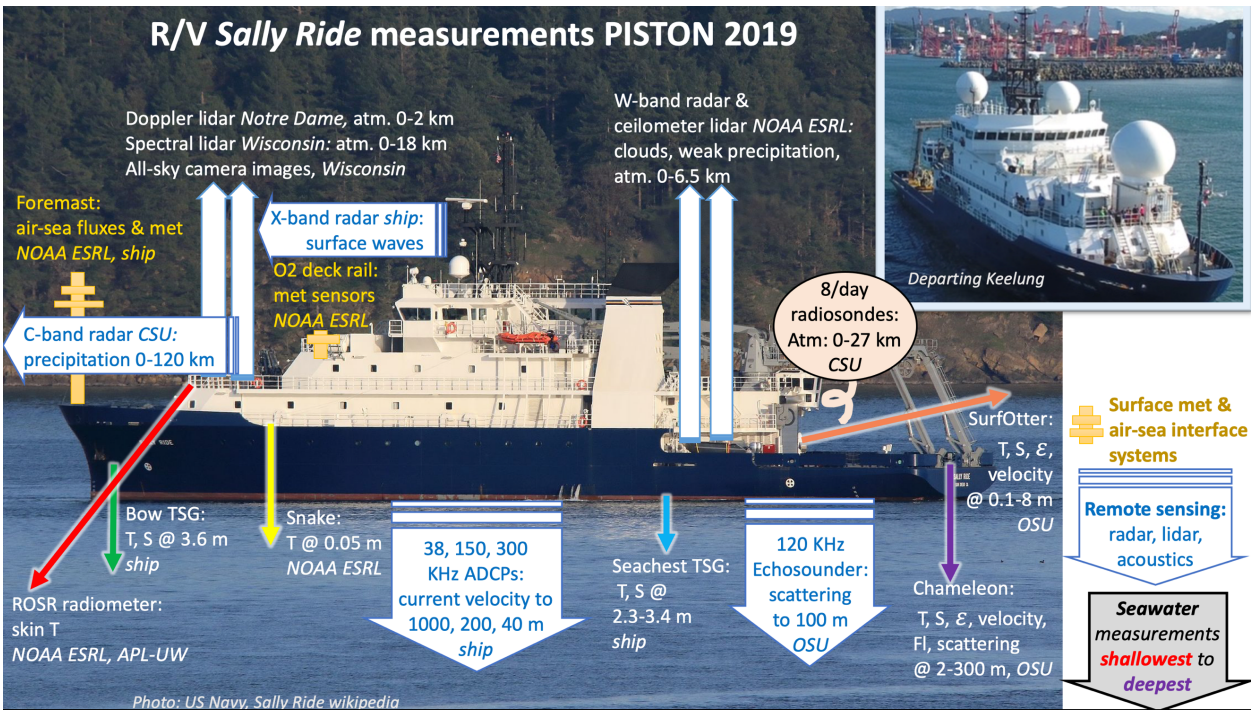

SCIENCE PARTY
Chudler Kyle CSU student
Clayton Adam CSU student
Dolan Brenda CSU scientist
George Jim CSU engineer
Hughes Kenneth Oregon St U Scientist
Hsiao Yu Cheng NTU student
Hsieh Hsin-Sung NTU technician
Hyde Orson Notre Dame U engineer
Latham Kerry Oregon St U engineer
Logan Josh Oregon St U student
Lu Yuanzheng Oregon St U Scientist
Moulin Aurelie Oregon St U Scientist
Moum Jim Oregon St U Ch.Sci.
Razenkov Igor U Wisconsin engineer
Rocque Marqui CSU student
Thompson Elizabeth NOAA ESRL scientist
Vutukur Pavan Oregon St U engineer

Figure 1 - Sally Ride from NASA P3 operating E of Luzon

This is a brief report of PISTON 2019 field ops. Data shown have not been quality-controlled.

Introduction

PISTON 2019 was scheduled to operate W of Luzon. This was canceled since MSR to operate in Philippines EEZ was denied by Philippines DFA. Operating region was redefined to international waters to the Philippine Sea E of Luzon within flight range of NASA aircraft from Clark aircraft base near Manila operating in support of the CAMP2Ex field program.

R/V Sally Ride (SR) departed Keelung, Taiwan 02Sep2019 as TC Lingling traveled N approaching Taiwan. The decision to depart Keelung harbor was made to avoid being ordered to evacuate the harbor in the case that the path of Lingling intersected Keelung. SR made way straight E to 130E to avoid the TC before entering ops area. Operations were interrupted (17-21Sep) by Invest 95W that ultimately became TC Tapah. Overboard instrumentation was recovered and SR moved to 15N 128E. In total, 5-1/2 days were lost to weather.

SR scientists were in continual contact with CAMP2Ex (NASA aerosol aircraft compaign). Brenda Dolan (CSU) was SR POC. The NASA Lear jet made 5 flights to SR and the NASA P3 made 3 flights to SR. Comms used: WhatsApp, WeChat and VHF.

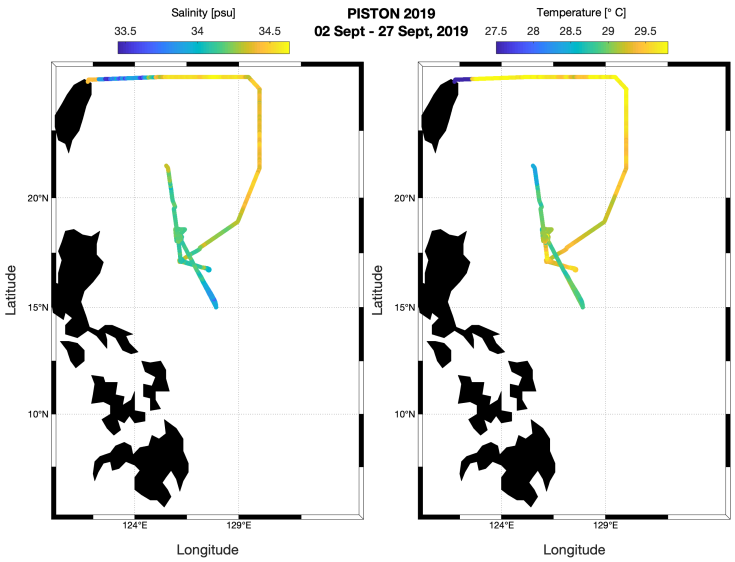

Figure 2 – Sally Ride ship track PISTON 2019

A summary plot of atmosphere-ocean temperature shows matching temperatures at the sea surface and decreasing away from it. Current/wind summary plots offer a few things to ponder and to discuss at Ft. Collins PISTON meeting November 2019.

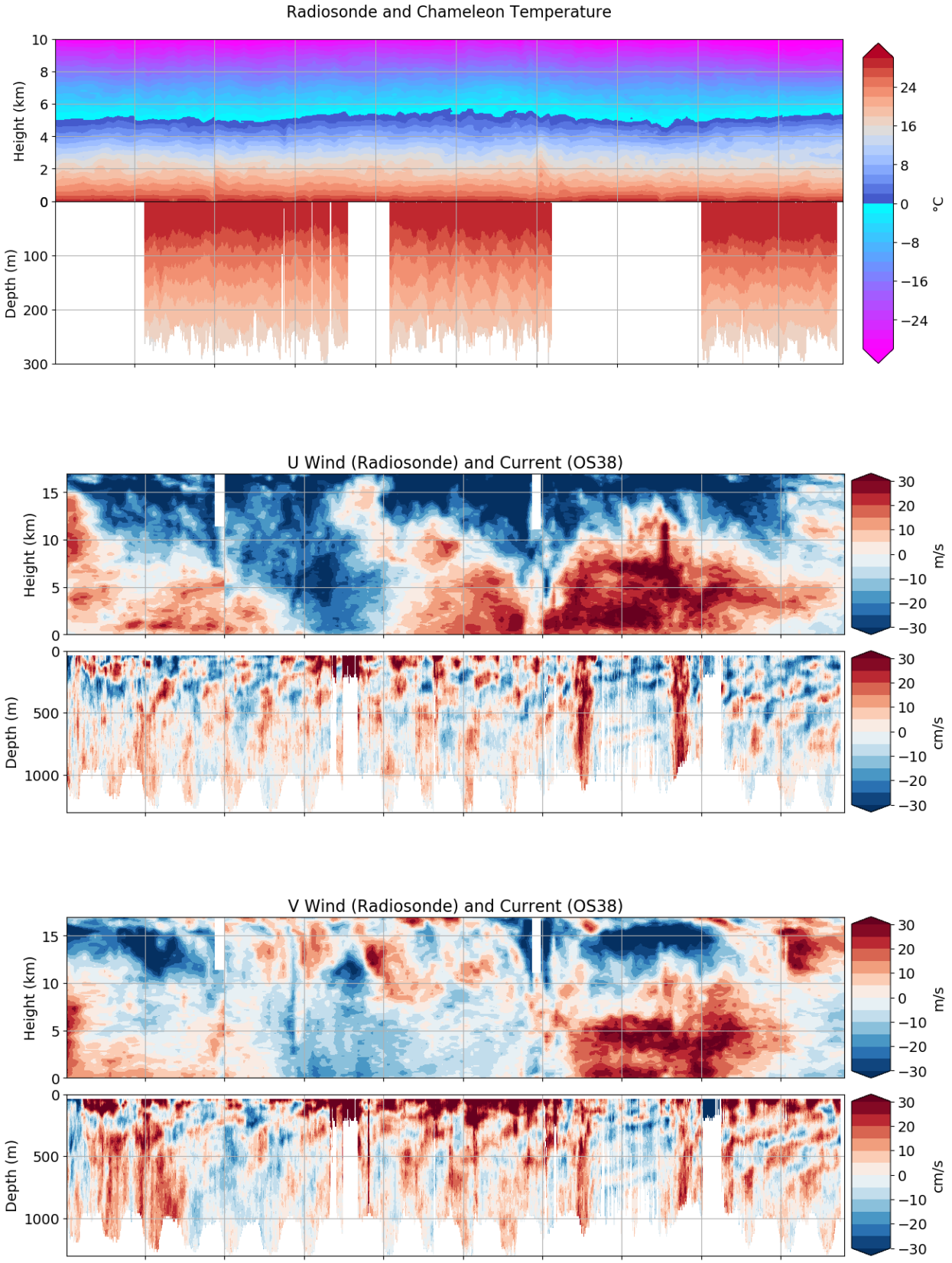
Radiosonde and Chameleon Temperature
Height (km)
Depth (m)
°C
U Wind (Radiosonde) and Current (OS38)
Height (km)
Depth (m)
m/s
cm/s
V Wind (Radiosonde) and Current (OS38)
Height (km)
Depth (m)
m/s
cm/s

PISTON 2019 SEA-POL and Sounding Report

Brenda Dolan, Kyle Chudler, Adam Clayton, Marqi Rocque, and Jim George

The CSU SEA-POL radar was built on the dock beside the Sally Ride over 3.5 days from 27 August to 1 September 2019. Final installation of the radar on the forward O1 deck occurred on 1 September. The location of the SEA-POL radar relative to the bridge and ship super structure resulted in a 80º blanking sector, allowing for a 280º view of port, bow and starboard relative to the ship (Fig. 1).

The SEA-POL scanning strategy was designed with three main objectives: 1) continuous near-surface rain mapping, 2) microphysics and lifecycle studies of convection, and 3) support of CAMP2Ex aircraft missions in the vicinity. During normal operations, a heartbeat of 10 minutes was selected which included a 3 minute rain volume scan with 7 elevation angles (Fig. 2) starting on the 10 minute, followed by 6.5 minutes of RHI "volumes". Such RHI volumes were selected by the radar scientist with the objective of capturing the lifecycle and microphysics of convection, and therefore the cells were "tracked" over their lifetime no matter if other things of interest were in the domain. Priority was given to cells and convection moving along a SEA-POL radial in order to maximize the ability to determine the flow structure, as well as allowing a single RHI angle to capture a consistent cross-section of the storm over time. Typically, these "volumes" included 4 azimuth angles that were repeated several times over the six minutes. Occasionally long-range surveillance scans, with range out to 300 km, were included to place the observations in context, understand contamination from second trip, and to determine what else might be lurking beyond SEA-POLs normal radius of 120 km. When the ship experienced light rain, bird bath scans were recorded in order to determine the Zdr bias, which was nominally found to be 0.3 dB, as in previous deployments. For CAMP2Ex missions, the rain mapping scan was discontinued in order to have the agility to work with the planes on a faster timescale. During these periods, small sector volume PPIs around the echo the planes were working were performed that took about 2 minutes. These were followed by RHI volumes on the same echoes to provide high-resolution vertical structure. Finally, a quick 360 surveillance scan was occasionally included in order to look for other potential targets for the aircraft. SEA-POL ran nearly continuously from the start of operations on 5 September through 08 Z on 25 September. At times, RHIs were ceased due to excessive rates of pitch and roll which would cause the antenna to dip below the minimum elevation limit. This primarily occurred on 21 September. During the cruise, over 39000 RHIs, 20000 PPIs, and 300 SUR scans were performed (Fig. 3). For CAMPEx, SEA-POL supported 5 Lear missions to the area and 3 P3 flights.

We found significant interference with the ship's HiSeas Net internet antennas. A test was performed on 7 September to characterize the interference. The ship rotated 45 degrees in heading every half hour, and the headings with good / bad interference were documented (Fig. 4). Headings from NNE to SSE experienced less RFI than west headings. With the help of the ship's IT professional, it was determined that the port side HiSeas Net antenna, also operating at C-band, had a direct line of sight to SEA-POL at those headings. If that antenna was pointed away from SEA-POL, the RFI cleared up. It was determined that this could be done for case studies (such as CAMPEx flights) for headings from 180-260 and internet would be preserved. Therefore, during CAMPEx operations, the ship was generally oriented between 0 – 266

degrees and the port antenna pointed away. This worked so amazingly that very light echoes such as gust fronts and boundary layer clouds could be detected by SEA-POL (Fig. 5)

Official operations began the morning of 5 September after 2 days of eastward transit to evade the influence of typhoon Lingling, and ended on 25 September at 12 Z during the transit back to Keelung. SEA-POL operated nearly continuously and without major issues for the entire duration. During this time period, SEA-POL observed five major precipitation events (Fig. 6). The "monsoon tail" of typhoon Lingling were sampled on 5 September, followed by a relatively quiet period with little rain or echo around the ship. A large mesoscale convective system moved through on 8-9 September, bringing several hours of precipitation and echo. The monsoon gyre 95W brought moisture to the domain 10-12 September, followed by a large MCS on 17 September which yielded the highest domain averaged rain rates of the cruise, over 1.75 mm/hr. Finally, as 95W spun up into tropical storm Tapah 20-21 September, SEA-POL sampled the outer rainbands. During the quiet periods, warm rain cells which largely remain below the melting layer height of 5 km were still ubiquitous, and sampled with many RHI volumes. Overall, SEA-POL sampled a wide variety of echoes, including non-precipitating boundary layer cumulus, shallow warm rain cells, isolated deep, electrified convection, and MCS-scale convection and stratiform regions (Fig. 7). Several interesting questions arose from these observations, including how can warm rain cells generate extremely large reflectivities (> 60 dBZ) and extremely large rain drops (>5 mm, 4+ dB ZDR)? Do these large drops form under certain sea states or environmental conditions? What is causing the scattering when SEA-POL can see oceanic boundaries such as gust fronts? What determines if a cell is able to become electrified? What is the microphysical structure of the stratiform region of an MCS over the ocean? What are the flow structures in all of these echoes?

SEA-POL and the Sally Ride supported 7 CAMPEx missions to the area. The P3 visited three times on 10 September, 22 September, and 24 September. However, convection was limited on these days so only a few cells were sampled within the SEA-POL domain. In addition to the joint mission with the P3 on 22 September, the Lear Jet worked convection near the Sally Ride four other times: 10, 13, 15 and 17 of September. During these days, the Lear and the Sally Ride worked together to find interesting targets for the Lear to fly though (Fig. 8). These ranged from shallow convection to warm rain and embedded convection.

To characterize the environmental conditions during the cruise, atmospheric soundings were launched every 3 hours beginning 6 September. During transit on 5 September, 4 balloons were launched at 0, 6, 12, and 18 UTC. Balloons were launched from the stern of the ship 30 minutes prior to 0, 3, 6, 9, 12 ,15, 18, and 21 UTC in order to center the profile at that time. However, during CAMPEx aircraft operations in the area, sondes were occasionally launched early, delayed, or in one case, skipped, per request of the aircraft pilots. During the cruise, 160 balloons were launched, with 3 sonde failures and 7 balloon failures (all failures were immediately relaunched). The resulting time-height series of the anomalies (as measured against the cruise mean) shows the different environmental influences experienced by the ship (Fig. 9). The middle of the cruise was anomalously hot and dry, with the winds shifting from easterly to westerly. In fact, the precipitable water reached a surprising minimum of 37 mm on 12 September 21 UTC. The developing Tapah brought more northeasterly winds and a moister troposphere around 17 September. The last week of the cruise was marked by a cooler but

drier upper troposphere, strong southeasterlies aloft and north westerlies near the surface. This period brought the lowest observed CAPE of 890 J/kg on 24 September at 06 UTC.

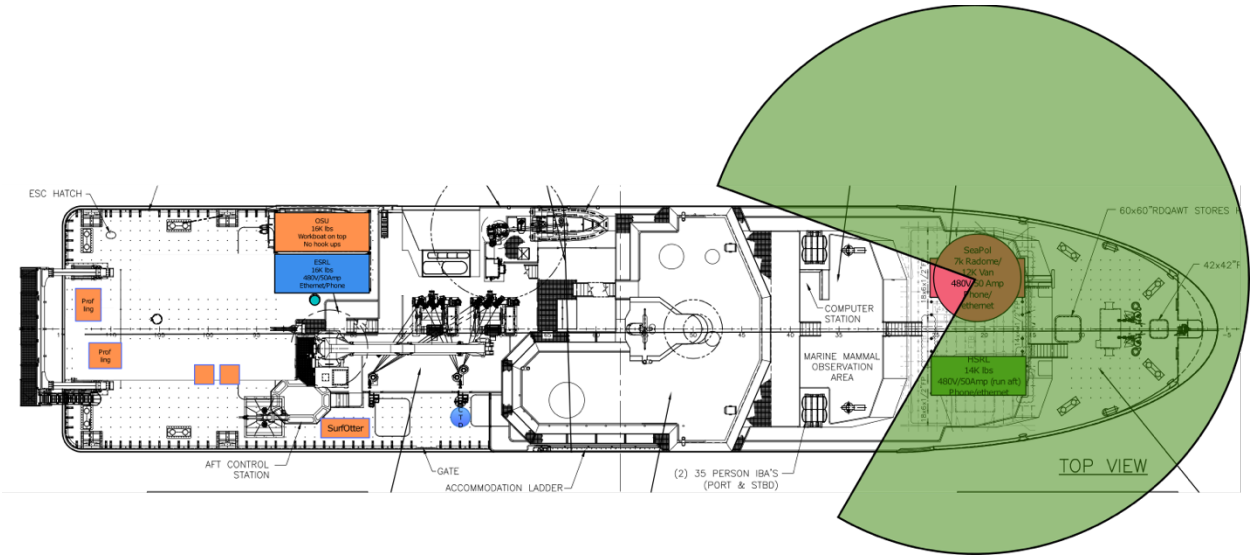

Figure 1: SEA-POL radar coverage area (green) on the Sally Ride.

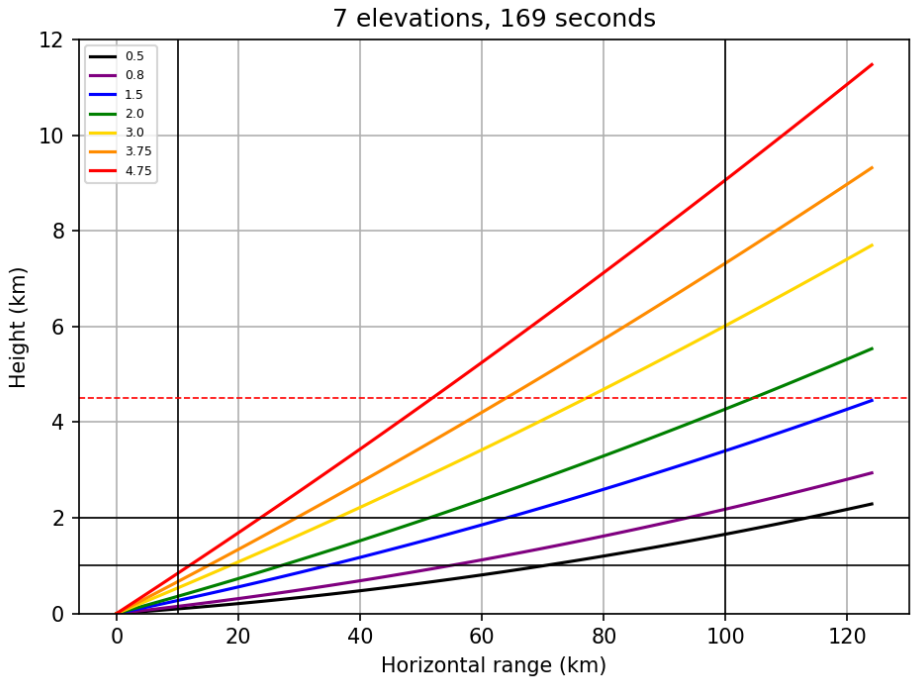

Figure 2: Elevation angles used in the PISTON 2019 rain mapping ppi volumes.

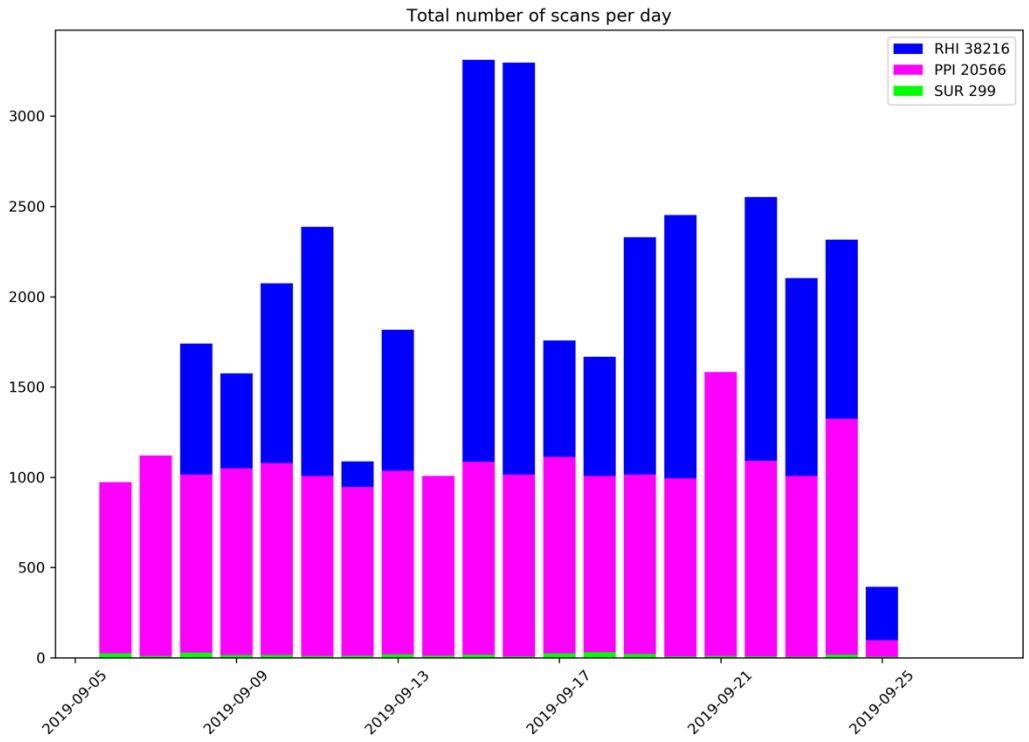

Figure 3: Breakdown of scan type per day of the cruise.

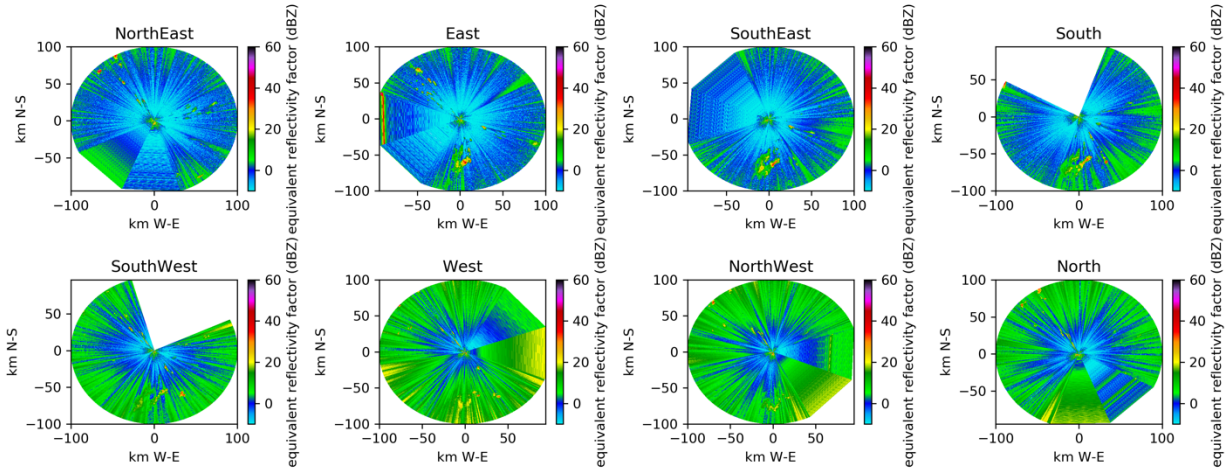

Figure 4: SEA-POL images as a function of ship heading. Note the RFI raises the noise floor about 10 dB, resulting in more green colors.

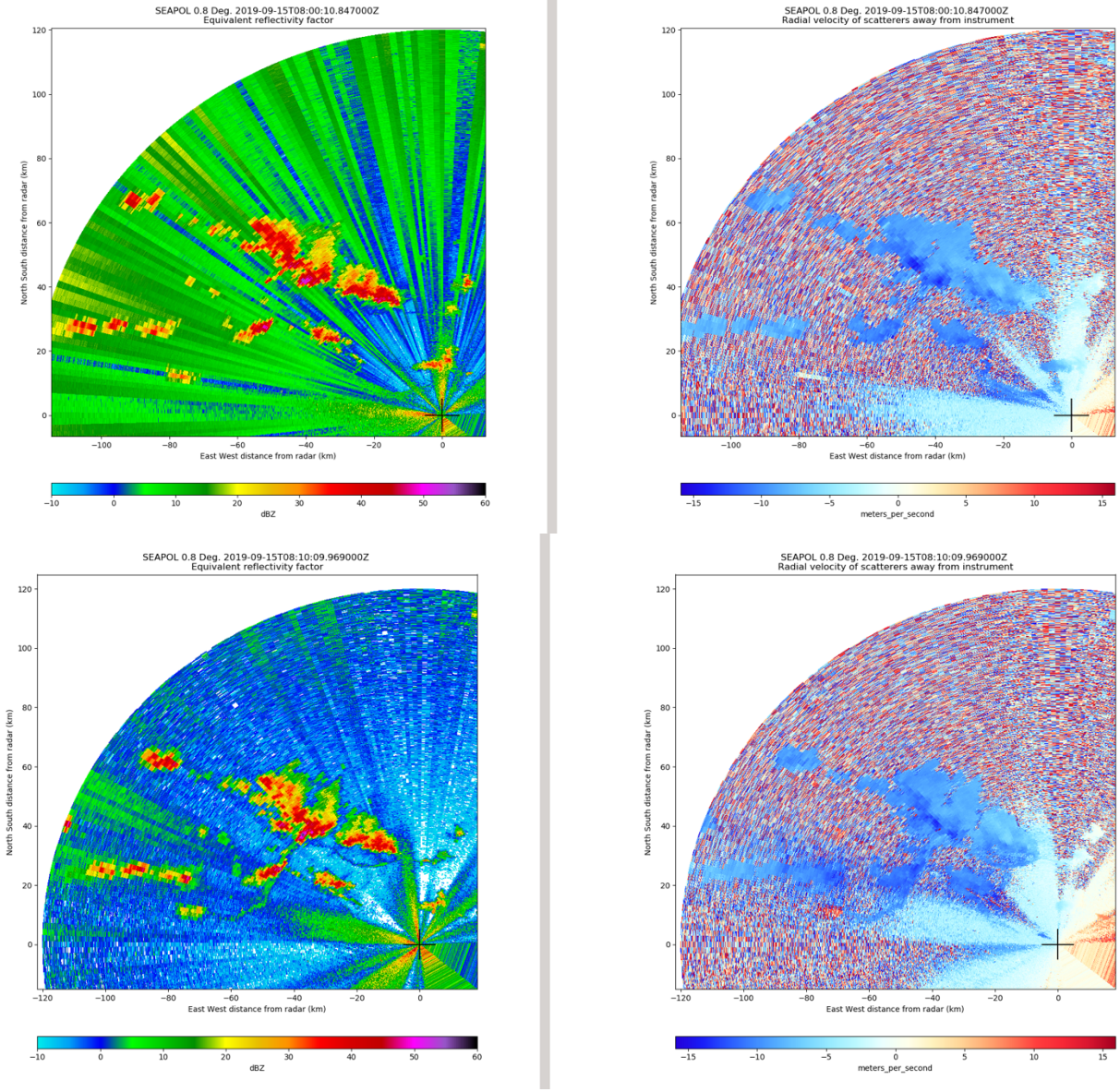

Figure 5: SEA-POL PPI with port HiSeas Net antenna in normal operations (top) and with the antenna pointed away from SEA-POL (bottom).

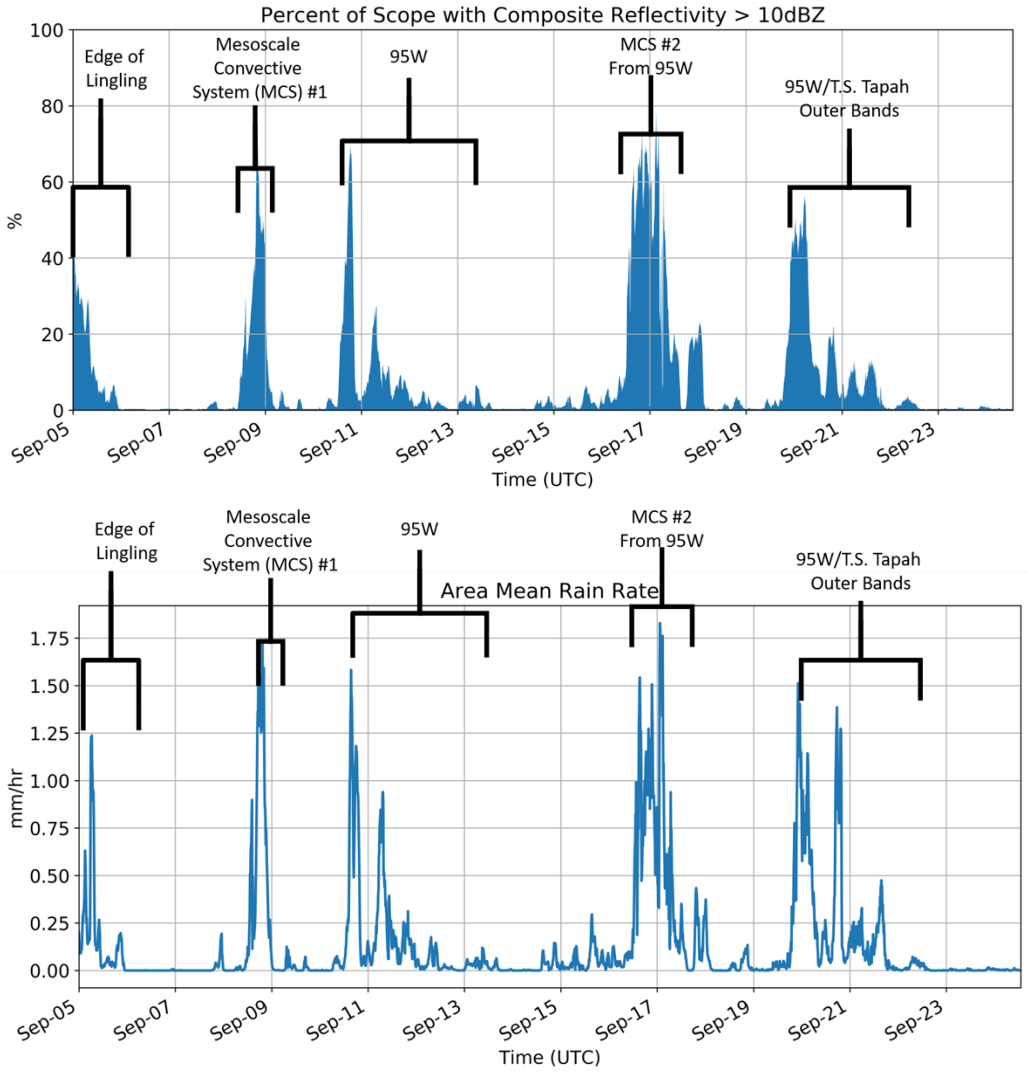

Figure 6: Timeseries of SEA-POL coverage area (> 10 dBZ; top) and domain mean rain rate (bottom).

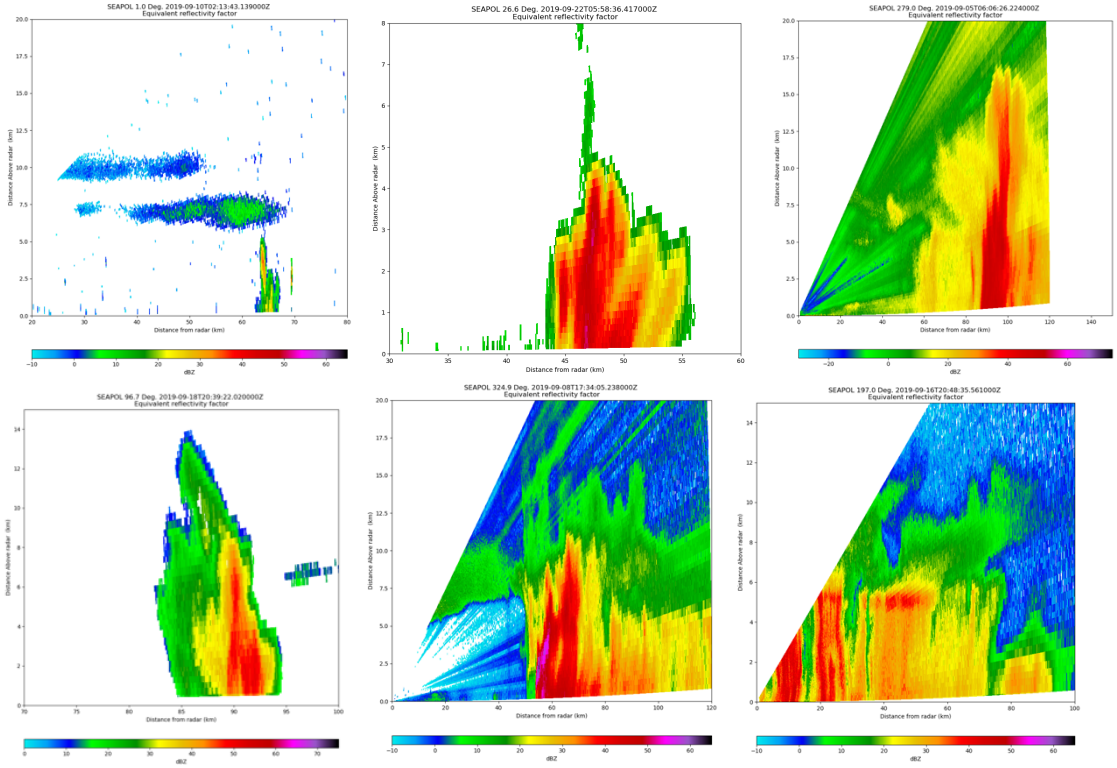

Figure 7: Reflectivity examples of clouds and shallow convection (top left), robust warm rain (top middle), isolated deep convection (top right), electrification (lower left), MCS convective line (lower middle), and stratiform rain (lower right) sampled by SEA-POL during PISTON 2019.

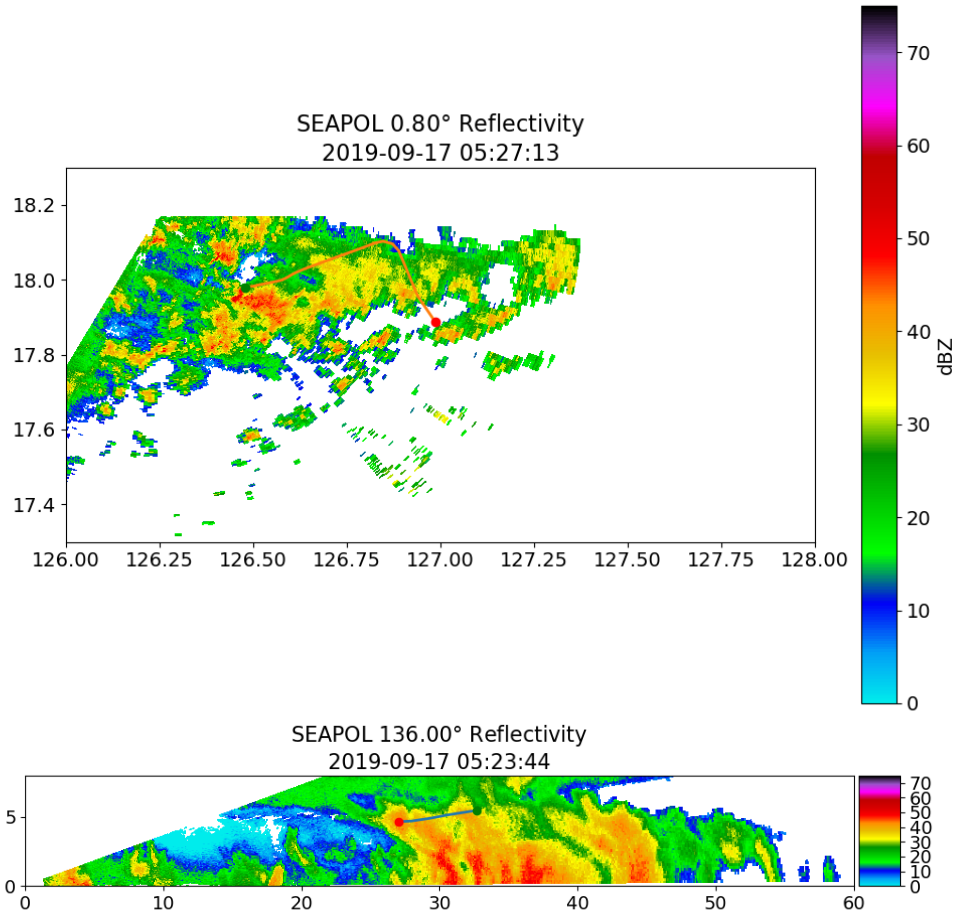

Fig. 8: Lear in convection at 0527 UTC (top) 0523 UTC (bottom). Green point indicates start and red the end point of the track during the approximate volume.

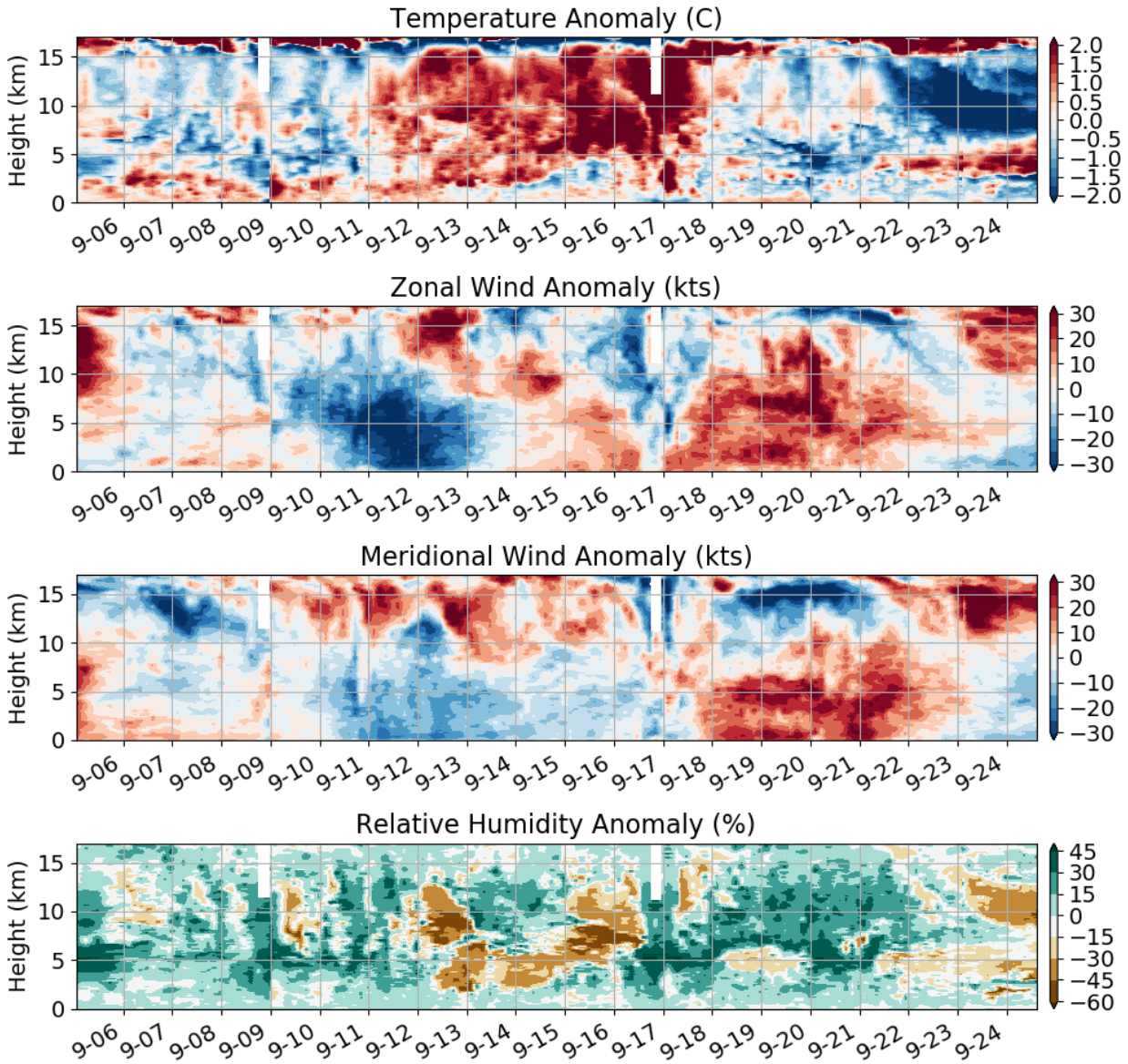

Figure 9: Atmospheric radiosonde time-height series of the cruise-averaged temperature (top), zonal and meridional wind (middle two), and relative humidity (bottom) anomalies.

PISTON 2019 report on measurements of air-sea fluxes, surface meteorology, clouds, and near-surface seawater

Elizabeth J. Thompson, NOAA ESRL PSD, elizabeth.thompson@noaa.gov

Personnel and Institution:

Elizabeth J. Thompson, Chris W. Fairall, Sergio Pezoa
NOAA ESRL PSD
Earth System Research Lab, Physical Sciences Division, Boulder, CO

Byron Blomquist, Ludovic Bariteau
NOAA ESRL / CIRES
Cooperative Institute for Research in Environmental Sciences at U. of Colorado Boulder

Simon de Szoeke
Oregon State University, Corvallis, OR

Orson Hyde
U. of Notre Dame, South Bend, IN

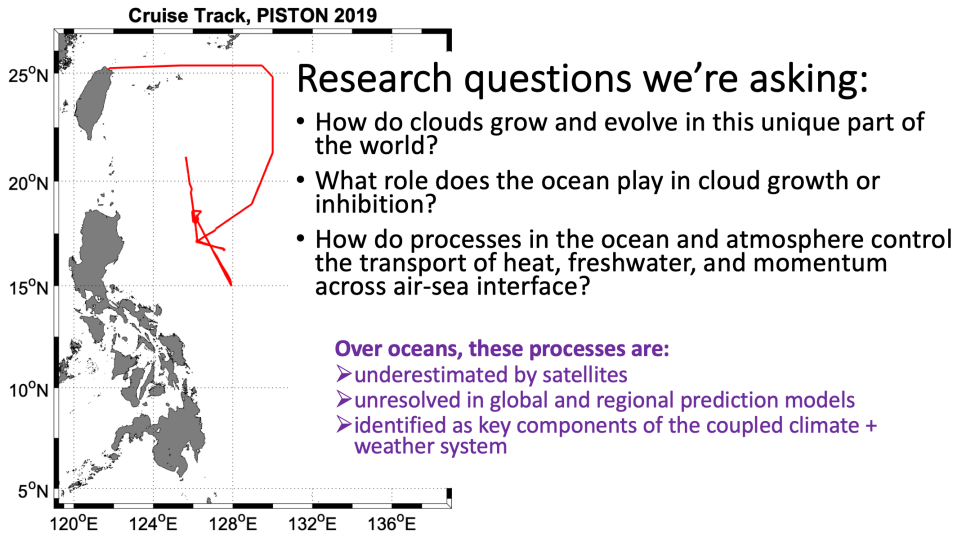

Timeline of ship operations in 2019:

- May 23 - May 27: Port call in Phuket, Thailand. Meteorological and flux instruments were installed on the O2 deck rail and the foremast prior to MISOBOB by B. Blomquist.
- May 27 - June 26 and July 6 - Aug 14: Equipment was operational for 2 cruises of the MISOBOB experiment in Indian Ocean. Port calls in Chennai, India. Data collection and preliminary data processing were run onboard by S. de Szoeke and O. Hyde. Final data processing run post-cruise by S. de Szoeke and B. Blomquist. Several data issues were present by completion of MISOBOB due to water leakage and some instruments being not plugged into UPS.

- Aug 25 - Sept 1: Port call in Keelung, Taiwan. Foremast lowered so that meteorological and flux instruments could be serviced by S. Pezoa. Several ethernet and serial cables were replaced due to water damage during MISOBOB, including for the sea snake and some foremast mast sensors. Configuration files for the heading, GPS, roll, and pitch were corrected. Desicants were replaced in IR and solar radiometers. All equipment was working properly at beginning of PISTON except for the second IR radiation pyrgeometer. The redundant, secondary met measurements made by the WXT system were not expected to be of great quality because of the placement of this unit over the O2 deck. W-band cloud radar and ceilometer were installed by S. Pezoa. Infrared radiometer (ROSR) was installed by E. Thompson
- Sept 2 - Sept 27 (total sailing time); 01 Z Sept 5 – 12 ZSept 25 (time sampling and saving data): Meteorological, flux, radiometer, and cloud instruments were operational for PISTON in Philippine Sea. Operated by E. Thompson. Every day at 01:30 Z, 09:30 LT, the Licor was sprayed with freshwater for about 1 min. Every day between 01:30 - 03:00 Z, the ceilometer lens was wiped with a clean dry paper towel, the radiometers were wiped with a clean wet and then clean dry paper towel, and the same was performed for the ROSR optical rain detector. The color of the desicants was periodically checked during the cruise. It remained purple-ish blue, so was not replaced.
- Sept 27 - Sept 29: Port call in Keelung, Taiwan. E Thompson and L. Bariteau removed all NOAA PSD equipment.

<u>Known data issues during PISTON:</u>

- The W-band radar was not turned on until yearday 253, Sept 10, at 2 Z due to mechanical issues.
- The W-band radar was shut down (data missing) when the P3 aircraft was within about 10 nm range. The P3 had a similar wavelength downward-looking cloud radar; they would have damaged each other if both in transmit/receive mode at the same time. A few other power faults occurred.
- The freshwater hose attached to the Licor on the main mast stopped working properly during PISTON, so the optical sensor was not clean enough to provide good data. Bad data are identified by times when AGC values > 55.
- The sonic anemometer had occasional data dropouts (reason currently unknown). In these cases, the ship's wind sensor data were used in the provided data file. The consequence of this is that turbulent (covariance) fluxes of heat, moisture, momentum were not computed during these times.
- The W-band radar's vertical resolution was much smoother and coarser when the automatic motion stabilization system was unable to run, which occurred when ship pitch and/or roll were > 7°. Due to the close proximity of the ship's smoke stack overhead and just forward of the W-band radar's field of view, the radar's motion stabilization system was electronically limited to $\leq 7°$ pitch and roll. In other words, the radar became immobilized in pitch, roll, or both directions when this limit was met. Typically, when the ship pitched and rolled, the radar will adjust its position in equal magnitude and opposite direction. If the ship rolled or pitched more than 7°, then the

radar's compensated position would have resulted in the transmitted radar pulse being reflected off of the metal smokestack. In this case, an excessively strong returned pulse to the radar would have destroyed its sensitive receiver. At times, the radar's position would be stuck at the limit switch position but the pitch would keep compensating, or vice versa. When either direction was compromised, the radar would get stuck in that position until this was discovered (no automatic detection or alarm was in place). Then its position was manually reset to vertical relative the ship, fixed in the ship's reference frame. The auto stabilization process was restarted in calmer conditions.

- One of the pyrgeometers for downwelling IR radiation (PIR1 or PIR2) was not functioning properly prior to PISTON. It was not fully understood why disagreement existed between the radiometers, or which one is correct. The PIR1 values were low compared to PIR2, calculated clear sky solar radiation, and the ship's PIR (which was also too low and noisy). For now, PIR1 is used in the dataset.
- A warm bias of about 0.12°C was determined to be present in the sea snake T record according to collocated measurements made by the ROSR and SurfOtter (OSU). The bias has been accounted for (corrected) in the provided dataset.
- Since the WXT system (additional met sensors) was not mounted in an ideal location on the ship, its measurements had relatively poor agreement and data quality compared to the foremast measurements made by the ship and NOAA PSD. The WXT measurements show signs of deck heating during the day and flow distortion around the ship. These measurements were not used in the provided dataset. They were collected for redundancy.
- WAMOS waves statistics from the ship's X-band radar were not correctly computed in the first 2/3 of the cruise because the wrong configuration file was being used by the ship's automatic processing system. The data will be reprocessed by Tom Cook (UCSD) following the cruise, then added to this dataset.
- The ROSR radiometer for measuring skin T was calibrated in June 2019 in Seattle, WA in a field test and bath calibration test by E. Thompson and the manufacturer, Mike Reynolds, RMR Co. The ROSR does not collect data when it is raining. If rain is detected by the optical sensor, the radiometer's shutter closes immediately. The shutter reopens 120 sec after rain is no longer detected. A few time periods of ROSR data are also missing due to time spent for in-field tests.
- The ship's meteorological measurements were of similar magnitude and sign as NOAA PSD, except for rain rate and humidity. Humidity was being calculated with the wrong calibration coefficients prior to day 267, Sept 24. Starting sometime on day 267, Sept 24, the values were in much closer agreement to NOAA's. Rain rate was calculated cumulatively by the ship. The sampling resolution of the instrument was only 0.2 mm per second, so the effective resolution in mm/hr is only 5 mm/h, relatively coarse. The ship's long wave radiation measurement was noisier (greater variance) and anomalously low at times, sporadically, but overall this measurement seemed acceptable in most cases. The seawater measurements from the ship were biased by
    - the heating of the ship (sensors are inside the ship, not in the open ocean water)
    - flow distortion around the hull (the extent of which is unknown)

- temporary dropouts in pump flow rate due to exposure of to air. The portside aft seachest vent's pump took in air and lost its prime when rolls were high, which was relatively infrequent. The bow pump lost its prime relatively soon in the cruise due to excessive pitching (see below for more details). Data from TSGs was only considered good when 1.75 L/min > flow rate > 3.5 L/min. Values above and below these levels were discarded.

Summary of completed work:

- A 10-min time series was produced of the best meteorological data, seawater data, and computed air-sea fluxes from Sept 5 - Sept 25. The bulk fluxes were computed using the COARE 3.5 algorithm (Fairall et al. 1996a, 1996b, 1997, 2003, Edson et al. 2013). The raw data was also provided.
- Hourly plots of data from the W-band radar and ceilometer were also produced and posted. These show the evolution of clouds and the atmospheric boundary layer between 0-7.5 km height above sea level.
- All software used on the cruise was posted. The datasets and software will be updated after the cruise to produce the final dataset.

Work to be completed by end of 2019:

- Add time series data of significant wave height, wave period, and wave direction from ship's X-band radar WAMOS system. The data were collected on the cruise, but were processed initially with the incorrect configuration file. Tom Cook at UCSD will be reprocessing the data after we reach land.
- Add the zonal and meridional components of near-surface ocean current from ship ADCP measurements. Data is currently being processed by OSU. The data are collected from depths of about 15 – 40 m using the 300 KHz ADCP.
- Add zonal and meridional components of wind and wind stress.
- Determine which IR radiation measurement is best. PIR1 is used right now.
- The ship TSG measurements should be corrected to be consistent with the OSU SurfOtter, so that the TSG values relative to SST are consistent before and after the switch between bow and seachest water (see below).
- Determine the precise offset present in the sea snake T relative to Otter and radiometer. Update the dataset accordingly.

List of Instruments:

Table X: Table of NOAA ESRL PSD sensors. temporal sampling frequency and status.

NOAA sensor	**Frequency**	**Status**
Anemometer, sonic 3D, Gill	u,v,w winds @ 10 Hz	Functional with occasional dropouts
Motion Pack	accel. & rot. @ 10 HZ	Functional
Fast water vapor, Licor 7500	H_2O @ 10 Hz	Not functional
Bulk air T & RH, Vaisala	1 min avg	Functional
Rain rate, OSI ORG optical	1 min avg	Functional
Air pressure, Vaisala	1 min avg	Functional

Solar flux, Eppley PSP (2)	1 min avg	Functional
IR flux, Eppley PIR (1), Kipp Zonen (1)	1 min avg	Functional, but significant differences noted between sensors
SST, sea snake	1 min avg, 5 cm depth	Functional
Heading, GPS	10 Hz	Functional
Ceilometer, Vaisala CL31	15 sec avg profiles	Functional
W-band cloud radar	3 Hz profiles	Functional starting 02 Z, 10 Sept
Skin SST, IR radiometer	1 min avg, skin level	Functional

The type, purpose, manufacturer, model number, height above water line, and purpose are listed below where applicable

Foremast

Ship: (see SR19B.acq document)

- Aspirated Air T: RM Young, 41342VC, 15.24 m
- Aspirated Air Humidity: EE Elektronic, EE08, 15.24 m
- 2D Ultrasonic Wind Anemometer, RM Young, 86106, 15.24 m
- RM Young self-siphoning rain gauge model #50202, 15.24 m
- barometric pressure, RM Young, 61302V, 15.24 m
- solar and infrared radiometers. Eply PIR and PSP, 15.85 m
- surface PAR, Biospherical Instruments, QSR-2200, QSR-240P, 15.85 m ASL
- GPS, ship speed, heading

NOAA:

- temperature and humidity sensor, Vaisala, HMT 337, 13.75 m
- 3D sonic anemometer: Gill Instruments, Master Pro, 14.75 m
    - Measures turbulent components of air T and 3D components of wind
- open path licor gas analyzer, LI-COR, LI7500, 13.75 m
    - Measures turbulent component air humidity
- optical rain gauge, OSI Inc., ORG-815-DA, 13.75 m
    - Measures rain rate with higher precision than siphons or buckets.
- 6-axis motion detector system, Dystron and Donner, MP-1, 12 m
    - Used for correcting data for ship in roll, pitch, yaw

O2 deck starboard rail

- GPS and heading, 11 m
    - GPS System, Hemisphere GPS, VS-1000
    - GPS Antenna, Hemisphere, MDA30 and MDA10
- pyrgeometer, one Eppley PIR & one Kipp & Zonen IR PIR, 11 m
    - measures downwelling IR radiative flux
- pyranometer, two Eppley solar radiation sensors, PSP, 11 m
    - measures downwelling Solar radiative flux

- upwelling IR flux calculated as function of derived skin T of ocean and downwelling IR flux
- upwelling Solar flux calculated as function of downwelling Solar and assumed albedo = 0.955
- Vaisala WXT520, RM Young aspirator with sensor and fan, 11.31 m
    - aspirated weather station measuring humidity, temperature, rain, wind
- shielded pressure sensor, Vaisala SPH10, 10.39 m
    - Measures barometric pressure, accounts for dynamic P component from motion and wind

Aft:

- Motion stabilized vertically-pointing W-band radar on aft main deck. Designed and built by NOAA ESRL PSD (Ken Moran, Sergio Pezoa, Chris Fairall). Reference: Moran et al., 2012 - see specifications of radar listed in table to side. Peak power: 1.75 KHz. Measures cloud vertical structure, drizzle, and light to medium rain < about 10 mm/h between heights of 150 m - 6 km above sea level. 30 m vertical gate spacing. Continuous sampling in time. Motion stabilization is automatically adjusted to true vertical when ship pitch and roll <= 7°. Otherwise, the radar either got locked at a large angle temporarily or reset to vertical relative to the ship, fixed in the ship's reference frame. The W-band is sensitive to both cloud droplets and drizzle. When clouds are precipitating, it is not simple to determine the height of cloud base because it is difficult to distinguish cloud from precipitation. Radar signal is attenuated in medium to heavy rain > 10 mm/h. Signal gets extinguished above portions of cloud with rain drop characteristics that exceed this level. The motion stabilization system measures the roll, pitch, and heave of the radar platform, and attempts to mechanically redirect the pointing angle of the antenna in real time.

TABLE 1. Specifications of the PSD W-band radar for CalWater-2 flights.

Parameter	Value
Radar operating frequency (GHz)	94.56
Radar operating wavelength (mm)	3.17
Number of range gates	150
Range resolution (m)	25
Distance to first range gate (m)	489
Distance to last range gate (m)	4214
Number of Doppler velocity bins	128
Doppler velocity bin resolution ($m\,s^{-1}$)	0.12
Nyquist velocity ($m\,s^{-1}$)	7.68
Number of spectral averages	9
Minimum detectable SNR (dB)	−20
Minimum detectable reflectivity at 1 km (dBZ)	−34
Dwell time per average spectrum (s)	0.3
Antenna diameter (m)	0.305
Antenna gain (dB)	46
Antenna beamwidth (°)	0.7

    - Measured variables as function of height and time:
        - Radar reflectivity: Z, dBZ
        - Doppler velocity: V, m/s
        - Spectral Width: SW, m/s
        - Signal to Noise Ratio: SNR, dB
    - Measured variables as function of time:
        - heave of platform (vertical velocity), m/s
        - roll of platform, °
        - pitch of platform, °

  - Known data artifacts:
    - horizontal bands of brighter SNR and SW, potentially due to noise.
    - vertical banding of V due to ship motion. Will be corrected in future.
    - Coarse data resolution when motion stabilization couldn't be run in high seas

- Vaisala CL31 ceilometer lidar on aft Focsle deck. Measures backscattered reflectivity from 0-6 km above sea level with vertically pointing optical laser (lidar). Sensitive to gradients in refractive index. Data are used to derive time series of cloud base height and cloud fraction. Cloud bases are accurately detected when no rain occurs. Measurement is attenuated in precipitation, so less usable in this case. Ceilometer does not produce a reliable measurement of cloud base top; W-band should be used for that instead. Specifications of ceilometer?
  - Measured variables as function of height and time:
    - backscattered intensity
  - Calculated variable as function of time
    - cloud base heights at multiple levels, if multiple are detected
    - number of cloud layers detected in vertical dimension
    - Fraction of beam width obscured by cloud at each level

Port Rail:

- sea snake on Focsle deck: seawater T at depth of 5 cm, 0.05 m
- ROSR: Remote Ocean Surface Radiometer. A KT-15 infrared radiometer is contained in a system built by RMR, Co. in Seattle, WA. Deployed on port O1 deck. Measures 5 min average of skin T of ocean across a 1 m x 1 m area. Because of the wavelength used by ROSR, this measurement is not affected by atmospheric water vapor or aerosol absorption. Note: skin T of seawater is also derived from COARE 3.5 algorithm using the 10-20 cm depth measurement from sea snake as input.

Ship seawater:

- Surface gravity wave statistics made by WAMOS X-band marine radar system. Contact: Tom Cooke UCSD.
- thermosalinigraph SBE45: seawater T and S taken from both the underside of bow and aft engine room. Exact flow distortion around ship's hull, and subsequent mixing, is unknown. Please see data contained in readme below and figures below.

Readme file for air-sea fluxes near-surface seawater, and surface meteorology

_flux_readme_PISTON_2019.txt

PISTON 2019, Philippine Sea
Preliminary in-field dataset for air-sea fluxes, surface seawater, and meteorology
NOAA Earth System Research Lab Physical Sciences Division (NOAA/ESRL/PSD)

Values are either measured directly or estimated by COARE 3.5 algorithm
Please acknowledge:
NOAA/ESRL/PSD: Chris Fairall, Elizabeth Thompson, Sergio Pezoa
NOAA ESRL / CIRES: Byron Blomquist
Oregon State University: Simon de Szoeke

References for COARE 3.5 algorithm: Fairall et al. 1996, Fairall et al. 2003, Edson et al. 2013

Dataset is subject to change as updates, corrections, and more data become available
Please contact Elizabeth Thompson if errors are found or if changes/additional variables are requested.

Contact: elizabeth.thompson@noaa.gov

Note: * the signs of fluxes are oceanographic convention
negative = out of ocean, cooling the ocean
positive = into the ocean, warming the ocean
* the signs of wind are meteorological convention
direction = the direction wind came from

Fields in Matlab structure called "f", and columns in .txt file

t matlab date and time
yday year day = t - datenum(2019,1,1,0,0,0);
Lat decimal latitude
Lon decimal longitude
sog speed over ground, m/s
cog course over ground, deg
head heading, deg
wspd_15m true wind speed measured on foremast at 14.75 m ~ 15 m, m s^-1
wdir_15m true wind direction measured on foremast at 14.75 m ~ 15 m, m s^-1
wspdrel_15m relative wind speed measured on foremast at 14.75 m ~ 15 m, m s^-1
wdirrel_15m relative wind direction measured on foremast at 14.75 m ~ 15 m, m s^-1
U10N wind speed adjusted to 10 m height and neutral air stability, m s^-1
Psl sea level pressure, mb
skinT skin T of seawater measured by IR radiometer (ROSR), missing in rain
SST sea surface T = snake T - calculated cool skin - 0.12 deg C correction
qs sea surface specific humidity, g kg^-1, calculated from SST
Tsnake snake T at about 0.05 m
dT air-sea T difference = SST - T10N, deg C
dq air-sea q difference = qs - q10N, g kg^{-1}
T10N air T adjusted to 10 m height and neutral air stability, deg C
q10N air q adjusted to 10 m height and neutral air stability, g kg^-1
RH10N relative humidity adjusted to 10 m height and neutral air stability, %
rhoa air density calculated with 10 m values
skin_dT estimated T difference across cool skin, deg C
skin_dz estimated thickness of cool skin, m
hs sensible heat flux, W m^-2
hl latent heat flux, W m^-2
E evaporation rate, mm h^-1
ustar friction velocity in air, m s^-1
tau stress, N m^-2
IRdn downwelling infrared flux, W m^-2
IRup upwelling infrared flux, W m^-2
IRnet net infrared flux = IRdn + IRup, W m^-2
Solardn downwelling solar flux, W m^-2
Solarup upwelling solar flux, W m^-2
Solarnet net solar flux = Solardn + IRup, W m^-2
IRdn_clear calculated downwelling IR flux assuming no cloud cover, W m^-2

Solardn_clear calculated downwelling solar flux assuming no cloud cover, W m^-2
P precipitation rate, mm h^-1
hr rain heat flux due to T difference between rain drops and SST, W m^-2
hnet net heat flux = Solarnet + IRnet + hs + hl + hr
Ttsg seawater T measured by main lab TSG, deg C (see below for details)
Stsg seawater S measured by main lab TSG, PSU (see below for details)
Ftsg seawater flow rate measured by main lab TSG, L/min (see below details)
Ctsg seawater C measured by main lab TSG, mS/cm (see below for details)
Sigtsg seawater sigmaT measured by main lab TSG, mS/cm (see below details)
ID_Ftsg seawater flow rate ID for main lab TSG: 1 = good, 0 = bad
bad = find(F < 1.75 L/min or F > 3.5)
IDtsg 0 = bad tsg data during switch, 1 = before switch, 2 = after switch

Notes about seawater measurements from ship TSG:

ship bow intake = starboard hole at 3.6 m depth, 0.3-0.6 m forward and below bow thruster vent, feeds into bow thruster room.

seachest intake = port vent between 2.3-3.4 m depth, 0.6-0.9 m aft and just above bilge keel, feeds into engine room.

TSG 1 on ship's .MET files = TSG located in bow thruster room (SBE45).
At beginning of cruise, this TSG sampled bow water through a direct line.
After switch, this TSG re-sampled sea chest water after TSG #2.

TSG 2 on ship's .MET files = TSG located in main lab... which is used in this dataset
At beginning of cruise, this TSG re-sampled bow water after TSG #1.
After switch, this TSG sampled seachest water through a direct line.

The switch in plumbing happened between 23:30 Z on 11th and 00:20 Z on 12th because the bow was pitching so much in rough seas that the bow pump was losing its prime and taking in air. For remainder of cruise, we decided to use sea chest water (TSG#2) instead of the bow water (TSG#1).

Only data from TSG#2 are included herein.
9/11/19 23:30 Z when ship's TSG started to change from bow water to seachest water
9/12/19 00:30 Z when ship's TSG completed change from bow water to seachest water

Readme file for ceilometer cloud statistics

_ceilometer_readme.txt

PISTON 2019, Philippine Sea
Preliminary in-field dataset for ceilometer Lidar

Please see readme files in this same folder:
specifications sheet for the Vaisala CL31 Ceilometer Unit.
photos of unit deployed on Sally Ride

Please acknowledge:
NOAA/ESRL/PSD: Chris Fairall, Elizabeth Thompson, Sergio Pezoa
NOAA ESRL / CIRES: Byron Blomquist
Oregon State University: Simon de Szoeke

Dataset is subject to change as updates, corrections, and more data become available
Please contact Elizabeth Thompson if errors are found or if changes/additional variables are requested.

Contact: elizabeth.thompson@noaa.gov

Processed data formats:

PISTON_2019_cloudbase_ddd.txt

raw output at ~ 15 second resolution with the following columns

1 jd_ceil decimal day of year at start of interval
2 cloudcode cloud detection code, as follows:
0 = clear sky
1 = one cloud layer detected
2 = two cloud layers detected
3 = three cloud layers detected
4 = totally obscured
5 = partly obscured but determined transparent
3 cloud1 base height of lowest layer, m
4 cloud2 base height of next highest layer, m
5 cloud3 base height of highest layer, m

PISTON_2019_ceilometer_hr_ddd.txt
PISTON_2019_ceilometer_10min_ddd.txt

stats computed from raw data at 10 min ahd hourly resolution

1 jd_hr/jd_10min decimal day of year at start of interval
2 cloud_cnt count of cloud detections in interval
(codes = 1-3)
3 obscured_cnt count of obscured detections in interval
(code = 4)
4 part_obscured_cnt count of partly obscured detections in interval
(code = 5)
5 cloud_tot count of total cloud detections, sum of
(sum of cloud_cnt and obscured_cnt)
6 frac_cld cloud fraction (codes 1-3), 0-1
7 frac_tot cloud fraction (codes 1-4), 0-1
8 clear_cnt count of clear detections in interval
(code = 0)
9 frac_clear clear sky fraction, 0-1
10 one_layer_cnt count of single layer detections in interval
(code = 1)
11 multi_layer_cnt count of multi-layer detections in interval
(code = 2,3)
12 hgt_median median cloud base height in interval, m
13 hgtsm1 18th percentile of cloud base height, m
14 hgtsm2 64th percentile of cloud base height, m

Figures:

NOAA instrumentation

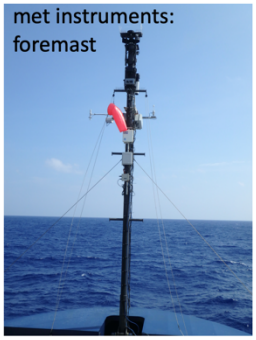

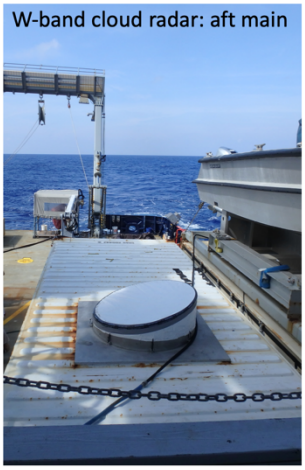

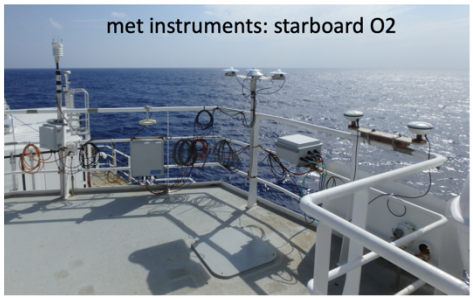

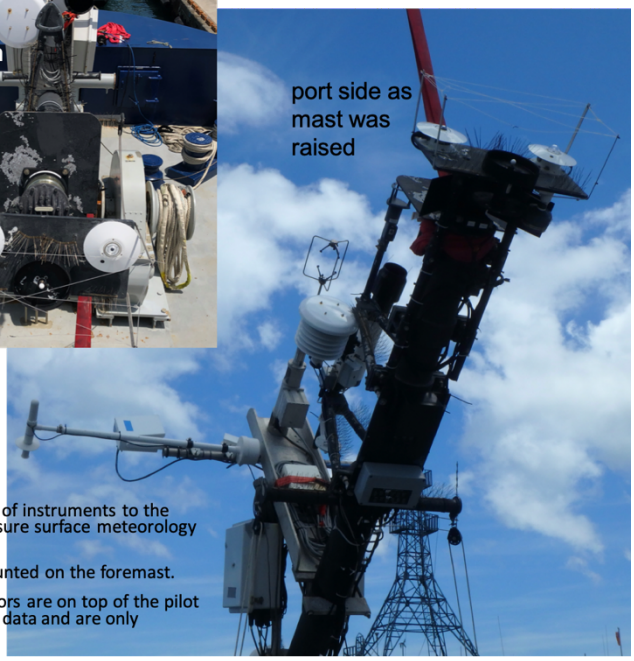

Foremast

- NOAA ESRL PSD added a full suite of instruments to the foremast and O2 deck rail to measure surface meteorology and air-sea fluxes
- The ship's met sensors are all mounted on the foremast.
- The ship has additional wind sensors are on top of the pilot house, but they are not recording data and are only available to the bridge

ROSR: The Remote Ocean Surface Radiometer

passively measures skin T with infrared radiation at ± 0.04-0.1 K accuracy

The 2°-wide beam dwells in 4 directions over 2-min to account for **sky reflection** and for 2-point **calibration** of IR brightness temperature

** No data when rain occurs*

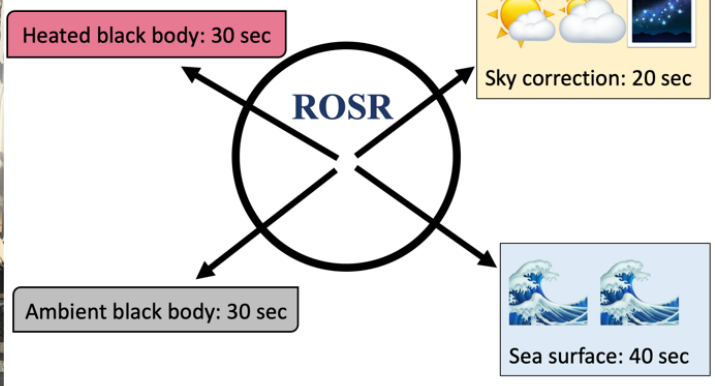

collaborative project between NOAA ESRL and APL-UW

Sea snake

simple, robust T measurement at 5 cm

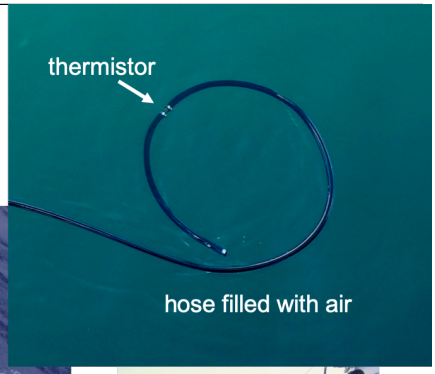

Hanging from port side focsile deck

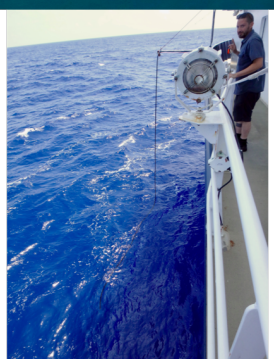

W-band radar: measuring the vertical structure and vertical velocity of clouds (raining and non-raining)

Clouds raining throughout troposphere

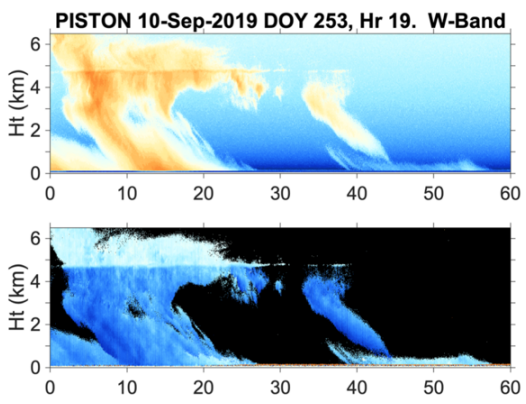

Non-raining clouds growing from the atmospheric boundary layer

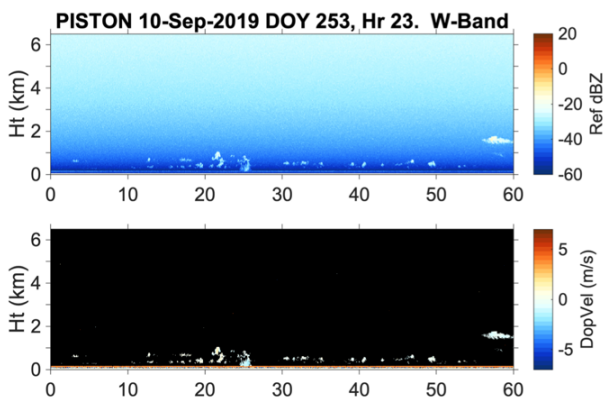

Ceilometer: a vertically-pointing lidar (laser of visible light) that detects refractive index gradients. Measures non-raining cloud base and depth of atmospheric boundary layer.

Backscatter is processed into time series of:

- Height of non-raining cloud base
- Intensity of cloud layer
- Depth of atmospheric mixed layer

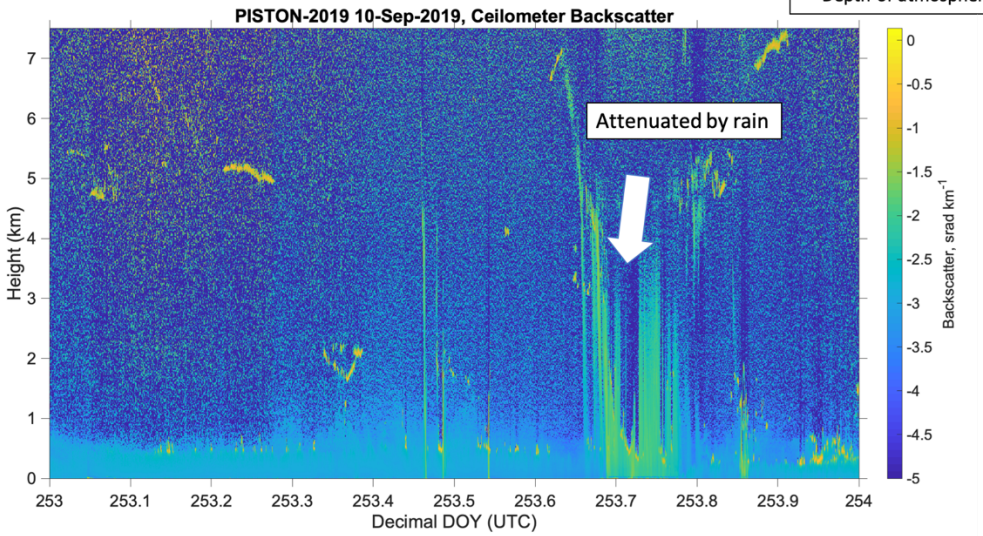

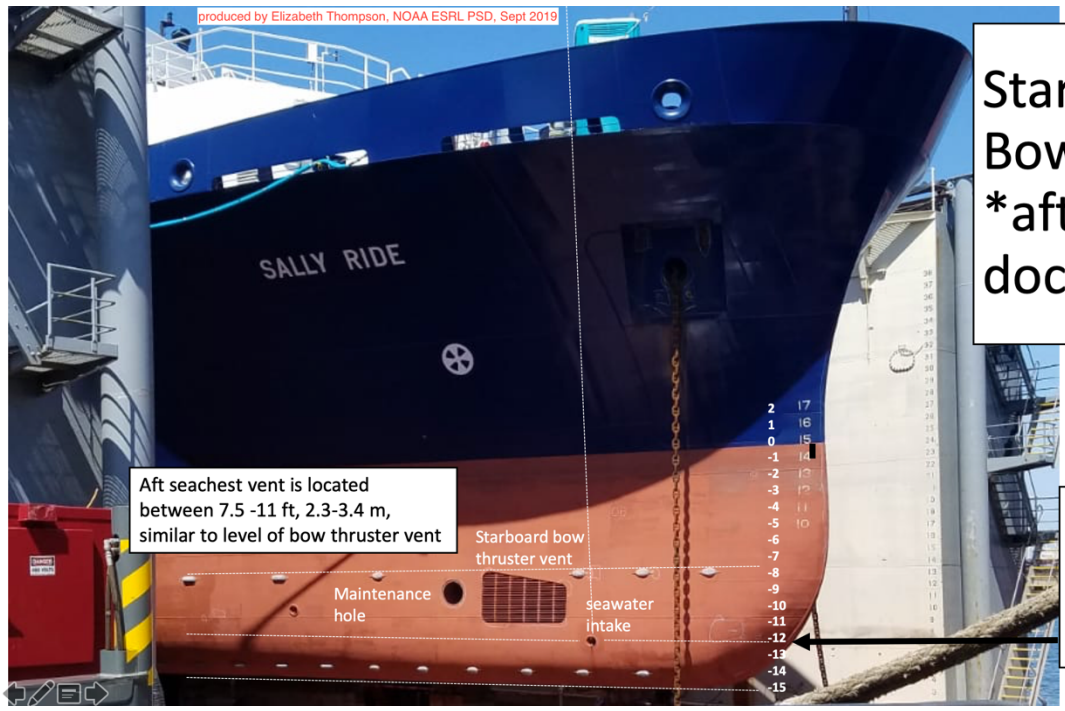
produced by Elizabeth Thompson, NOAA ESRL PSD, Sept 2019
SALLY RIDE
Starboard Bow *after dry dock
Aft seachest vent is located between 7.5 -11 ft, 2.3-3.4 m, similar to level of bow thruster vent
Starboard bow thruster vent
Maintenance hole
seawater intake
Bow seawater port is located at 12 ft, 3.6 m depth; 0.3 m ft below, 0.6 m forward of vent

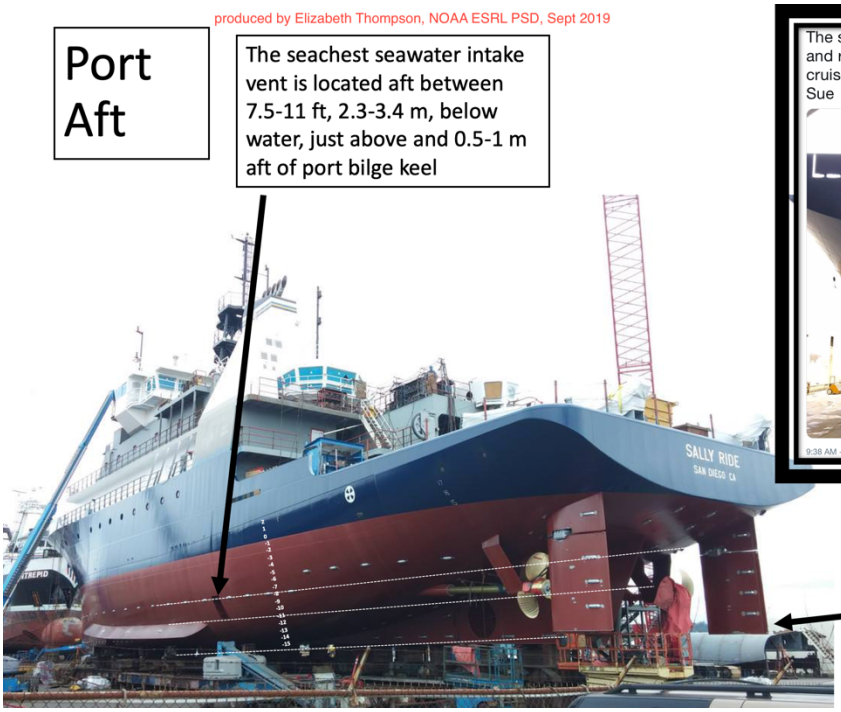
produced by Elizabeth Thompson, NOAA ESRL PSD, Sept 2019
Port Aft
The seachest seawater intake vent is located aft between 7.5-11 ft, 2.3-3.4 m, below water, just above and 0.5-1 m aft of port bilge keel
SALLY RIDE
SAN DIEGO CA
The base of the rudders are located at 14.5 ft, 4.4 m depth


The ship is in dry dock! It is getting upgrades and refits and will be ready for science cruises again soon. Photo by 2nd engineer Sue
SALLY RIDE
SAN DIEGO CA
9:38 AM - 17 Apr 2017
Twitter

Photos of ceilometer on Sally Ride for PISTON 2019. Aft Focsle Deck.

Photos of W-band radar on Sally Ride for PISTON 2019. Aft Focsle Deck. Next to smoking area, work boat, and ceilometer.

Preliminary Scientific Analysis:

The following time series show select output variables from meteorological, seawater, and flux data collection and preliminary processing. Notable to this dataset are the occurrence of several ocean diurnal warm layers, which warmed the sea surface temperature (SST), amplified the air-sea humidity and temperature gradients, and thereby accelerated the latent and sensible heat fluxes into the atmosphere. Despite low wind forcing, the sea surface heated and generated TKE in the atmospheric boundary layer. The strongest event was on 9/23, in which the SST warmed 2.5°C from sunrise to afternoon. During this time, the strongest values of the air-sea humidity gradients, sea surface specific humidity, and SST of the entire cruise occurred. When strong precipitation events occurred, atmospheric cold pools with gust fronts also amplified the air-sea T difference, which caused larger sensible heat fluxes into the

atmosphere. Also notable were a few extremely cloudy days that resulted in almost zero values of downwelling solar radiation. This occurred on 9/17 and 9/20. On these two days the net surface heat flux was negative all day (9/17) or only briefly positive (9/20), resulting in ocean cooling that is evident in the SST plots.

Please see readme above for more description of variables plotted below. dT = sea - air temperature difference (SST - T10) and same for dq for specific humidity. 10-m values of U, T, and q are for properties adjusted to 10 m reference height and for neutral atmospheric stability.

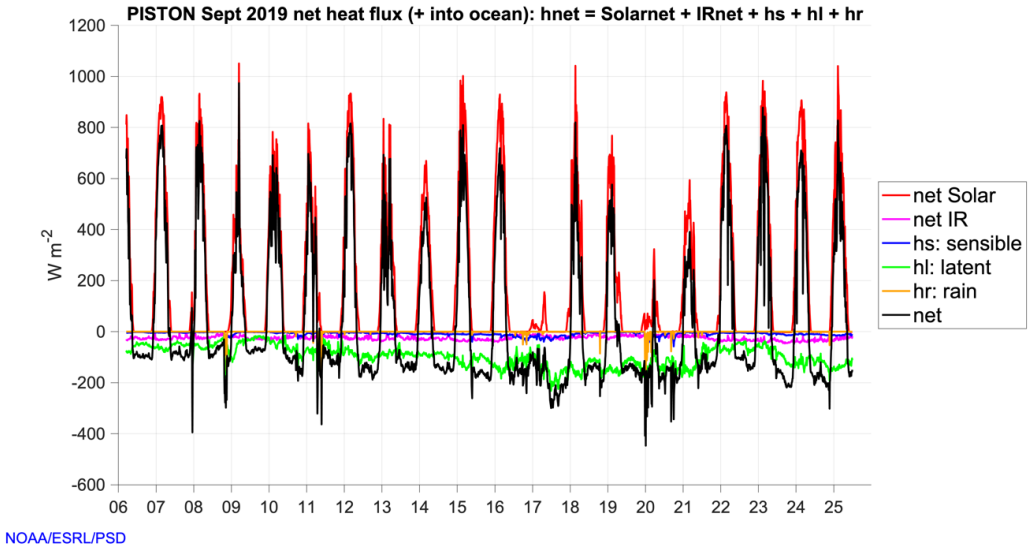

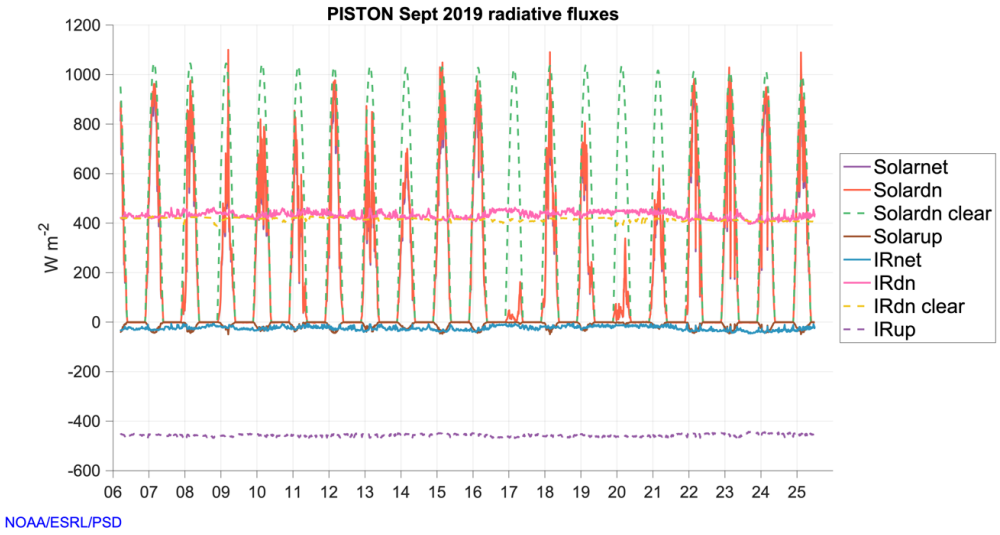

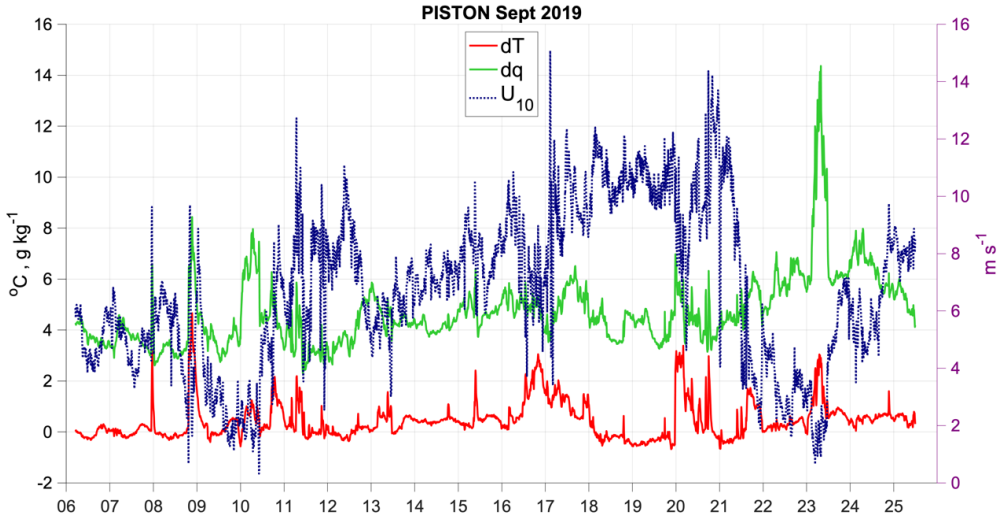
PISTON Sept 2019
dT
dq
U10
°C , g kg-1
m s-1
NOAA/ESRL/PSD

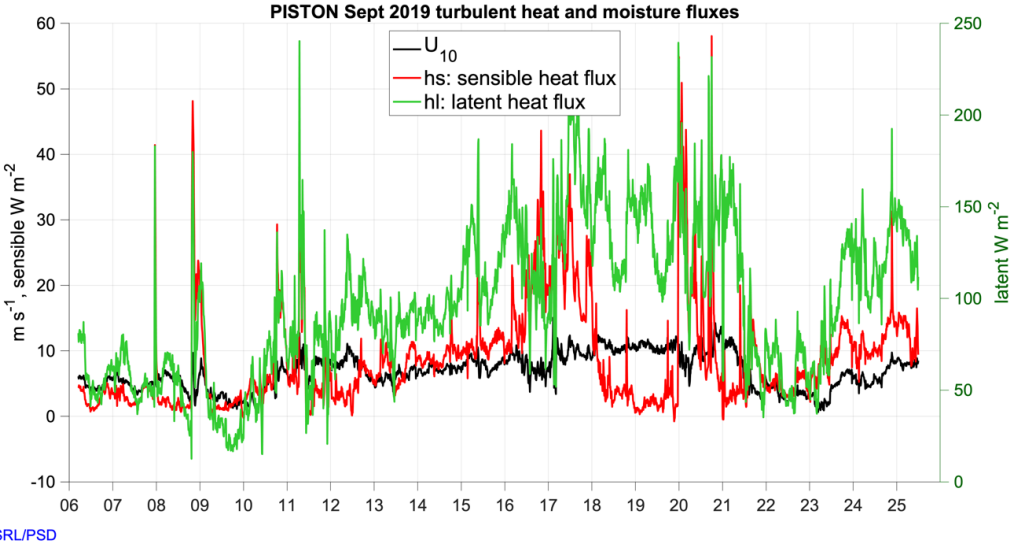
PISTON Sept 2019 turbulent heat and moisture fluxes
U10
hs: sensible heat flux
hl: latent heat flux
m s-1, sensible W m-2
latent W m-2
NOAA/ESRL/PSD

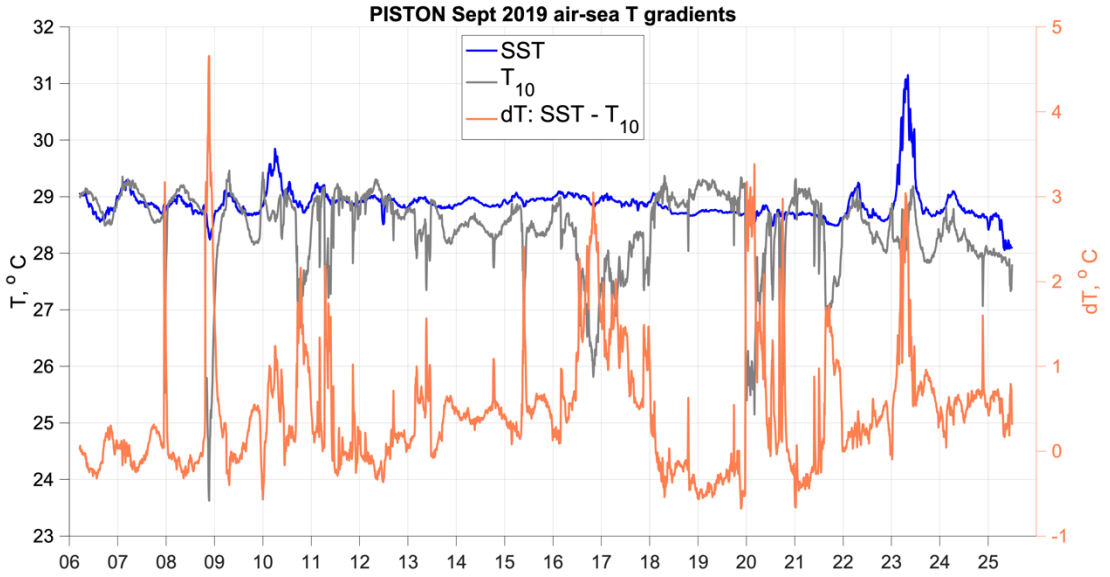
PISTON Sept 2019 air-sea T gradients
SST
T10
dT: SST - T10
T, ° C
dT, ° C
32
31
30
29
28
27
26
25
24
23
5
4
3
2
1
0
-1
06 07 08 09 10 11 12 13 14 15 16 17 18 19 20 21 22 23 24 25
NOAA/ESRL/PSD

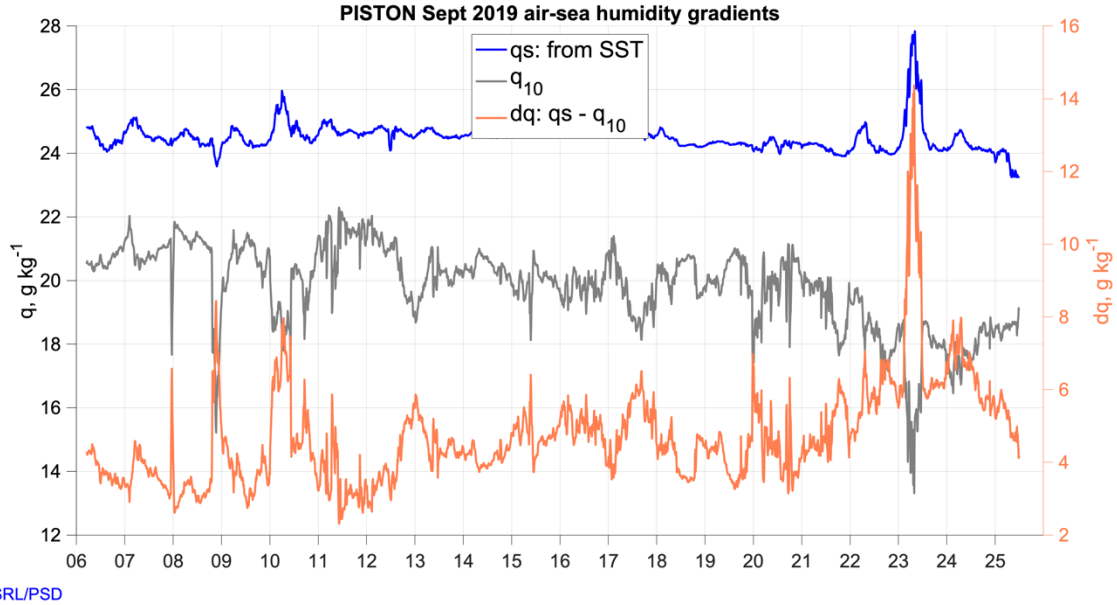
PISTON Sept 2019 air-sea humidity gradients
qs: from SST
q10
dq: qs - q10
q, g kg-1
dq, g kg-1
28
26
24
22
20
18
16
14
12
16
14
12
10
8
6
4
2
06 07 08 09 10 11 12 13 14 15 16 17 18 19 20 21 22 23 24 25
NOAA/ESRL/PSD

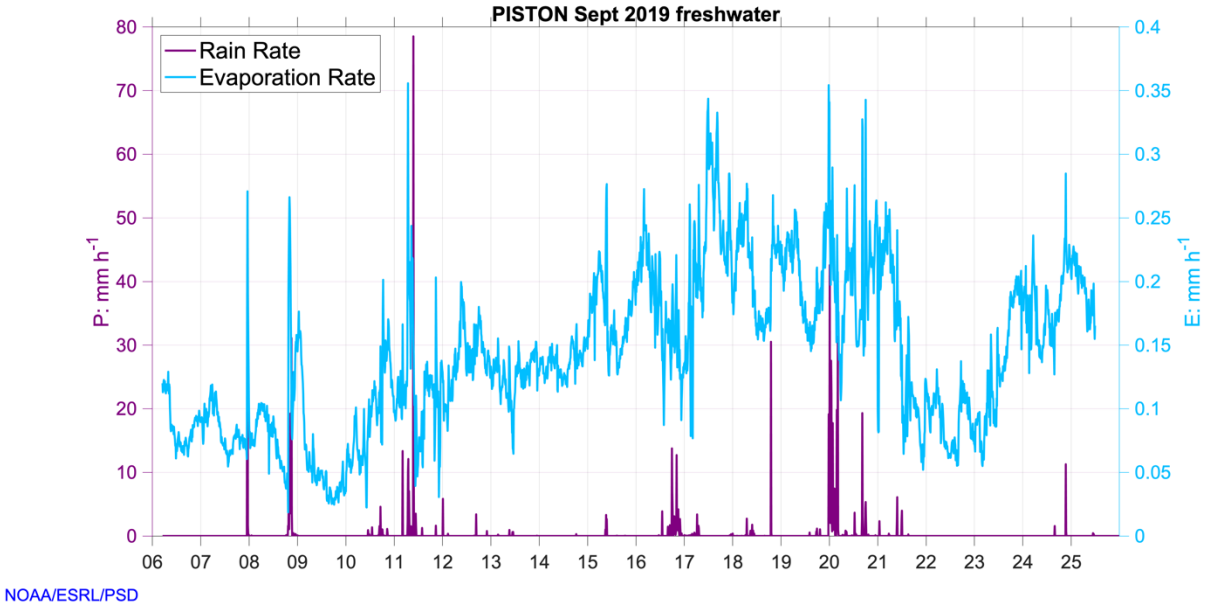
PISTON Sept 2019 freshwater
Rain Rate
Evaporation Rate
P: mm h-1
E: mm h-1
80
70
60
50
40
30
20
10
0
0.4
0.35
0.3
0.25
0.2
0.15
0.1
0.05
0
06 07 08 09 10 11 12 13 14 15 16 17 18 19 20 21 22 23 24 25
NOAA/ESRL/PSD

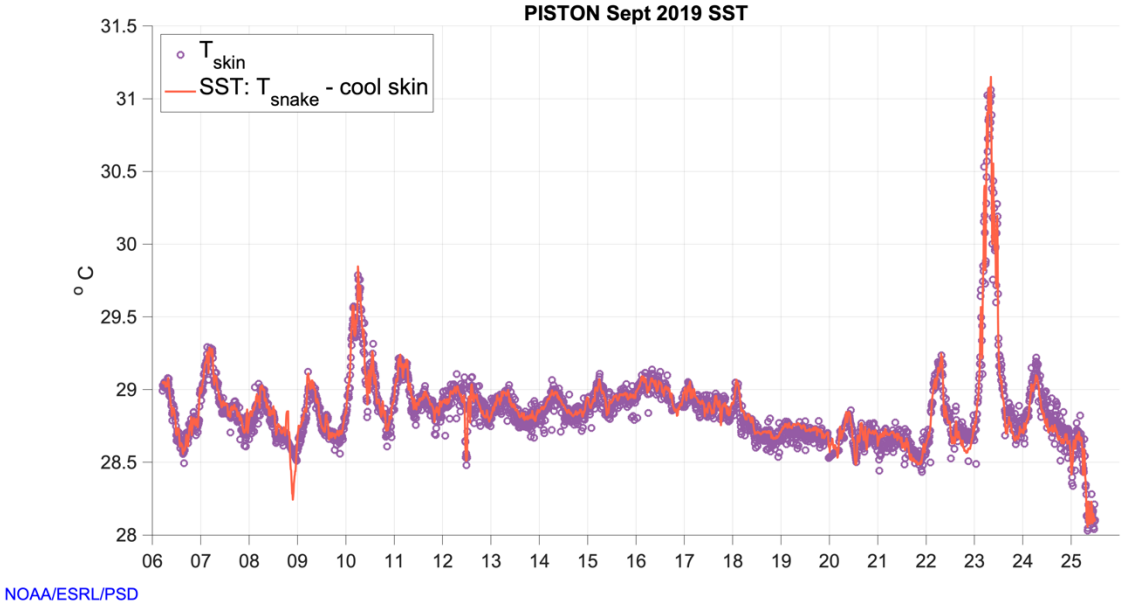
PISTON Sept 2019 SST
Tskin
SST: Tsnake - cool skin
° C
31.5
31
30.5
30
29.5
29
28.5
28
06 07 08 09 10 11 12 13 14 15 16 17 18 19 20 21 22 23 24 25
NOAA/ESRL/PSD

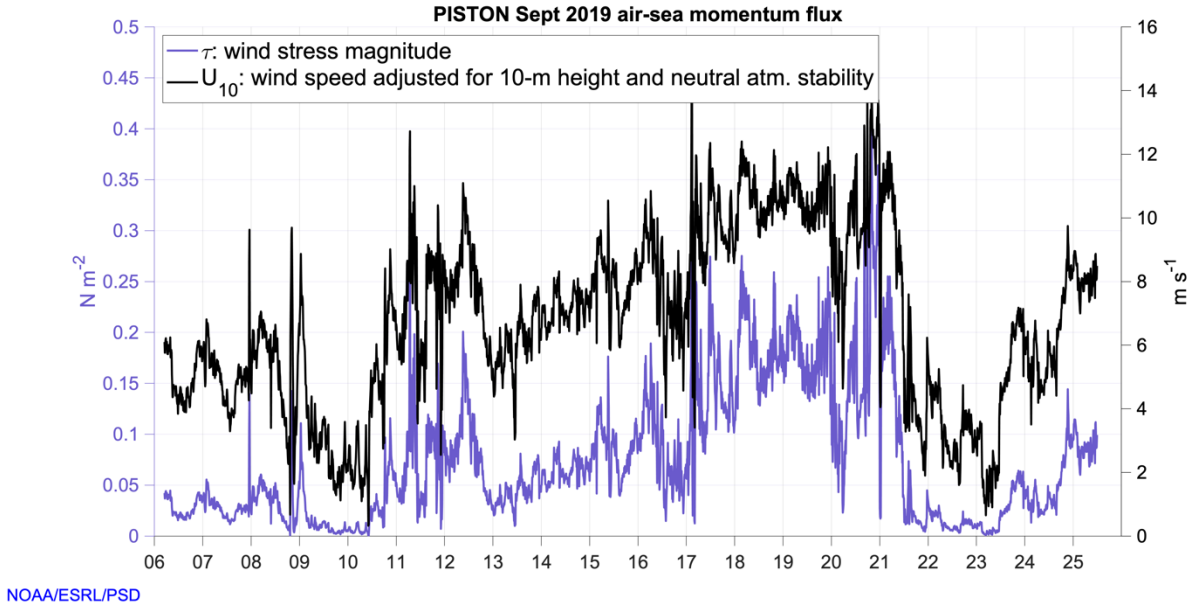

References:

Edson, J. B., Jampana, V., Weller, R. A., Bigorre, S. P., Plueddemann, A. J., Fairall, C. W., Miller, S., Mahrt, D., Vickers, & D., Hersbach, H. (2013). On the exchange of momentum over the open ocean. Journal of Physical Oceanography, 43(8), 1589–1610. https://doi.org/10.1175/JPO-D-12-0173.1

Fairall, C. W., Bradley, E. F., Godfrey, J. S., Wick, G. A., Edson, J. B., & Young, G. S. (1996). Cool-skin and warm-layer effects on sea surface temperature. Journal of Geophysical Research, 101(C1), 1295–1308. https://doi.org/10.1029/95JC03190

Fairall, C. W., White, A. B., Edson, J. B., & Hare, J. E. (1997). Integrated shipboard measurements of the marine boundary layer. Journal of Atmospheric and Oceanic Technology, 14(3), 338–359. https://doi.org/10.1175/1520-0426(1997)014<0338:ISMOTM>2.0.CO;2

Fairall, C. W., Bradley, E. F., Hare, J. E., Grachev, A. A., & Edson, J. B. (2003). Bulk parameterization of air-sea fluxes: Updates and verification for the COARE algorithm. Journal of Climate, 16(4), 571–591. https://doi.org/10.1175/1520-0442(2003)016<0571:BPOASF>2.0.CO;2

Moran, K., Pezoa, S., Fairall, C. W, Williams, C., Ayers, T., Brewer, A., de Szoeke, S. P., & Ghate, V. (2012): A Motion-Stabilized W-Band Radar for Shipboard Observations of Marine Boundary-Layer Clouds. Boundary-Layer Meteorol. (2012) 143: 3. https://doi.org/10.1007/s10546-011-9674-5

High Spectral Resolution Lidar (HSRL) and All-sky Cloud Images

Ed Eloranta eloranta@wisc.edu
Igor Razenkov

The High Spectral Resolution Lidar yields range resolved measurements of 532 nm backscatter cross section, extinction cross section, and depolarization as well as 1064nm attenuated backscatter cross section and depolarization. It is currently alternating between near vertical profiles and 0-15 degree rhi scans. Range resolution is 7.5 m, near vertical data is collected with 2.5 sec time resolution while the rhi data is collected at 0.5 second resolution. Depolarization allow discrimination between spherical particles(low depol) and irregular shapes (higher depol). Ratios between 532 and 1064 nm gives rough indication of particle size.

Sky camera images were also continuously collected.

UND Motion Compensated Doppler Lidar PISTON Cruise Summary

Jay Orson Hyde JayOrson.Hyde.17@nd.edu

The Lidar works in conjunction with the NOAA flux sensors installed on the mast and observation deck. Using a combination of vertical stares and six-part VAD scans every ten minutes. This scan strategy will, through further processing and analysis, give a value for vertical wind speed across the length of the beam, up to 2 Kilometers. For ship based deployments the Doppler Lidar is affixed to a custom made frame that will correct for the ship's motion on two axis and keep the Lidar level and the beam on target. In 2019 the motion correction frame conducted its' longest deployment to date. It has been supporting air/sea interaction research since June 2019 on board the RV Sally Ride, and evaluating the capabilities and endurance of the system has been an important part of Notre Dame Environmental Fluid Dynamics' mission this year. The system is quite reliable up to Sea State 2. During the deployment in PISTON sea state would occasionally be higher as the ship adjusted location to avoid tropical storms developing around the operational area east of Luzon. On September 16 the frame that was correcting for motion on the pitch axis failed, the frame was repairable and the Lidar was undamaged. Sea State was too high to restart the system until September 22nd. Scans continued uninterrupted until the end of research operations. In addition to researching the atmospheric physics between sea surface and the boundary layer, data gathered in 2019 will be used to speed up the workflow of integrating and correcting the datasets from the Doppler Lidar and Stabilization Frame. Plans for upgrading components and software of the motion correction system to allow longer endurance and the integration of other position sensitive sensors have been made based on the 2019 deployments.

Subsurface (Ocean) Measurements

Jim Moum, Kenneth Hughes, Aurelie Moulin, Kerry Latham, Pavan Vutukur, Josh Logan, Lu Yuanzheng (Oregon State University)
Hsin-Sun Hsieh, Yu Cheng Hsiao (National Taiwan University)
Orson Hyde (Notre Dame U)

Chameleon turbulence / CTD profiler – 200 m max depth
SurfOtter surface-following instrument platform / TC / Doppler sonar / turbulence upper 7 m
hull-mounted Doppler sonar (ADCP)
38 kHz (700m range)
150 kHz (250m range)
300 kHz (110m range)
Imaging acoustics 120 kHz echsounder
WAMOS wave radar

The principal focus of the OSU research for the 2019 PISTON field campaign was diurnal warm layer physics as this is what most directly feeds back to the atmosphere in the tropics during late boreal summer. Technical modifications to SurfOtter in early 2019 improved near-surface temperature, conductivity, turbulence and velocity measurements, permitting velocity profiles to within 1m of the sea surface. Chameleon extended the measurements from the near-surface to the longer-term thermocline (10-50 m depth) permitting complete observation of diurnal warm layer deepening.

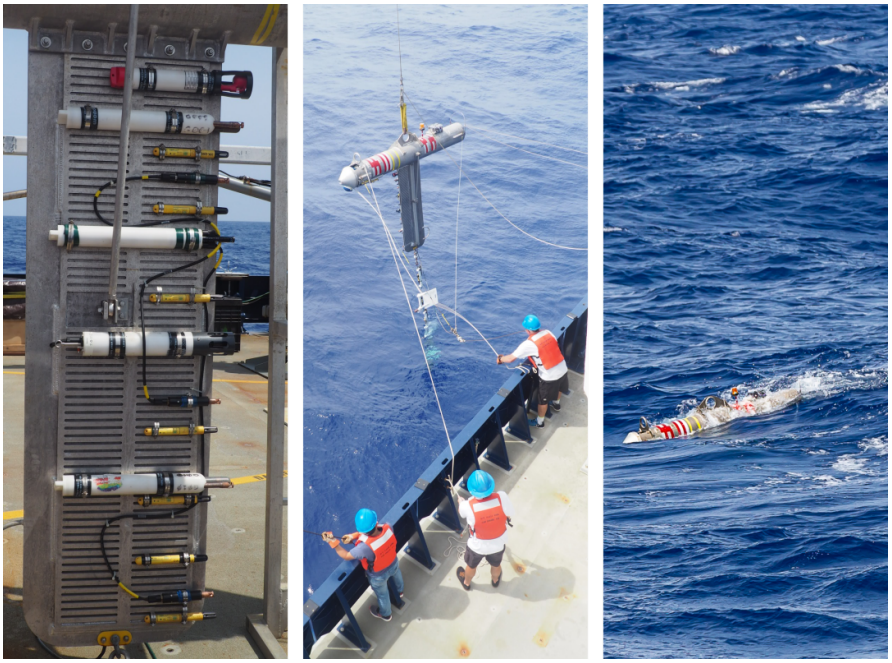

Figure 3 -SurfOtter deployment from R/V Sally Ride PISTON 2019

SurfOtter

The Oregon State University Mixing Group deployed the surface-following platform SurfOtter for a total of 12 days during the cruise. During this time, a wide range of conditions were sampled including a sunny day with winds persistently below 1 m/s, the remnants of a large storm with 8–10 ft waves and 15 m/s winds, and strong rain events with instantaneous rain rates exceeding 10 mm/hr. Consequently, the record includes the hot, fresh and slippery near-surface layers needed to assess the friction conveyed through them to the mixed layers beneath.

Deployments (times in UTC):

1. 07 Sep 0600–12 Sep 0800
2. 13 Sep 0820–17 Sep 0930
3. 21 Sep 0310–24 Sep 1110

During all three deployments, SurfOtter included the following instruments:

15 RBR soloT temperature loggers
Five CTDs (Seabirds, Idronauts, and RBR concertos)
Four GusTs (100 Hz fast thermistors together with a pitot tube, pressure sensors, and acceleromters)
A Tpod containing a further four fast thermistors
A Sentinel V 1000 kHz ADCP
A GPS unit

With minor exceptions, all instruments worked exactly as planned. Of particular note was the data obtained from the Sentinel ADCP. Following issues from PISTON2018 with interference from the fin, the ADCP placement was reconfigured, angled forward 30°. This enabled measurements of the near-surface velocity starting 0.8 m below the sea surface. An increase in velocity in the top few meters can be observed during days of strong insolation and weak-to-moderate winds. This process, termed a diurnal jet, has been inferred in previous studies. Here, we have been able to make the first direct measurements of the true depth-structure of the jet.

The eight fast thermistors on SurfOtter will enable a high-vertical resolution depiction of turbulence throughout the day. Combined with the observed velocity profile, we will be able to quantitatively establish the downward momentum flux from the wind and the consequences for dynamics of near-surface stable layers.

Accompanying figures show SurfOtter's ability to capture near-surface dynamics.

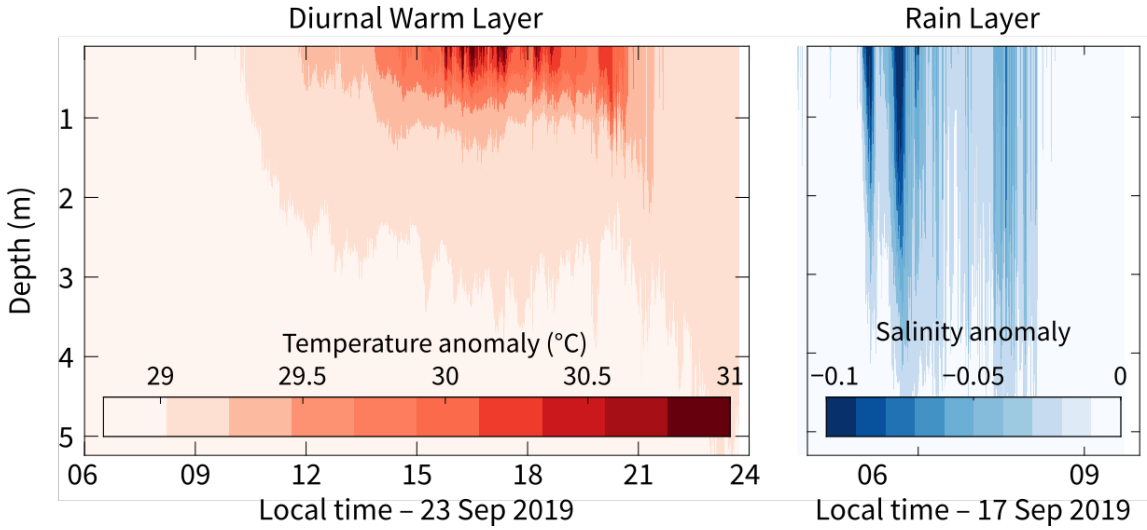

Figure 4 - Near-surface layers observed by SurfOtter. The diurnal warm layer occurred during periods of strong insolation and weak wind forcing. The rain layer occurred immediately following a strong rain event. Anomalies are relative to the deepest sensor at 5 m. The accompanying stratification traps a near-surface, wind-forced velocity jet. We might think of the left panel as a hot slippery layer and the right as a fresh slippery layer.

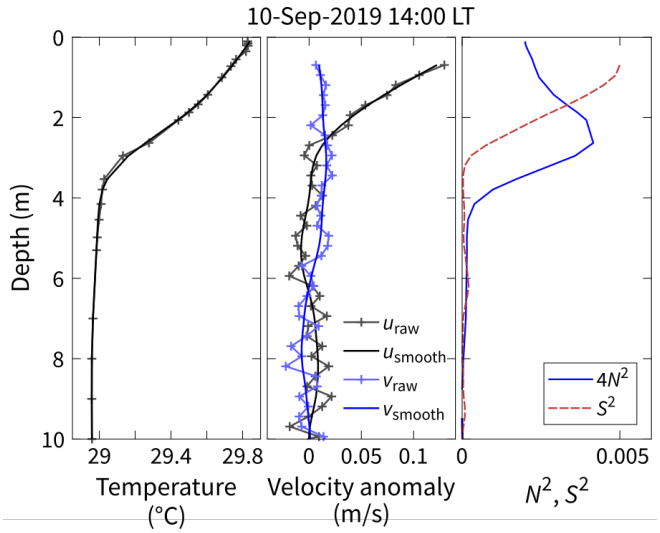

Figure 5 - Direct measurements of a near-surface diurnal jet at mid-day (14:00 LT). In this case, the stable, near-surface layer is accelerated by weak winds. This leads to shear-induced mixing in the top 2 m, suggested by squared shear (S^2) exceeding stratification ($4N^2$).

Chameleon / ADCP

Chameleon ops completely coincided with SurfOtter deployments. A simple summary is shown in the next figure followed by a brief discussion of two case studies.

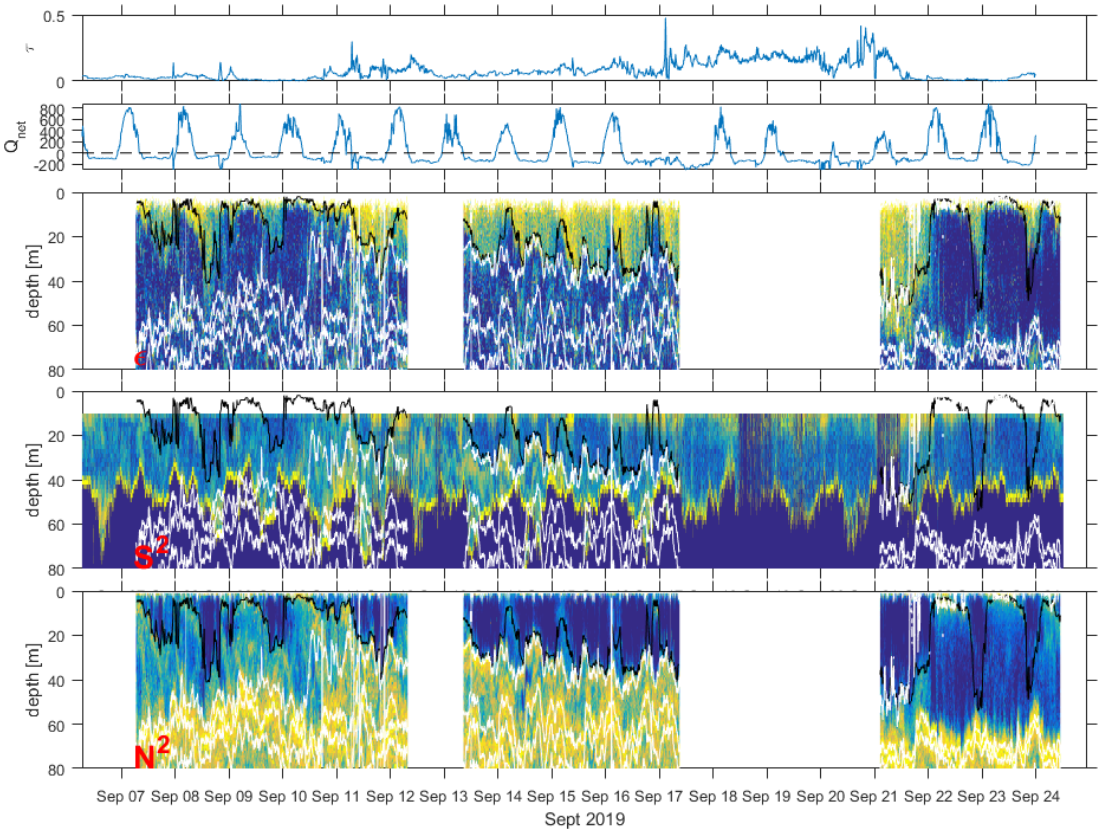

Figure 6 – Time series of wind stress, net surface heat flux, turbulence dissipation (ε), squared velocity shear (S^2) and stratification (N^2). PISTON 2019.

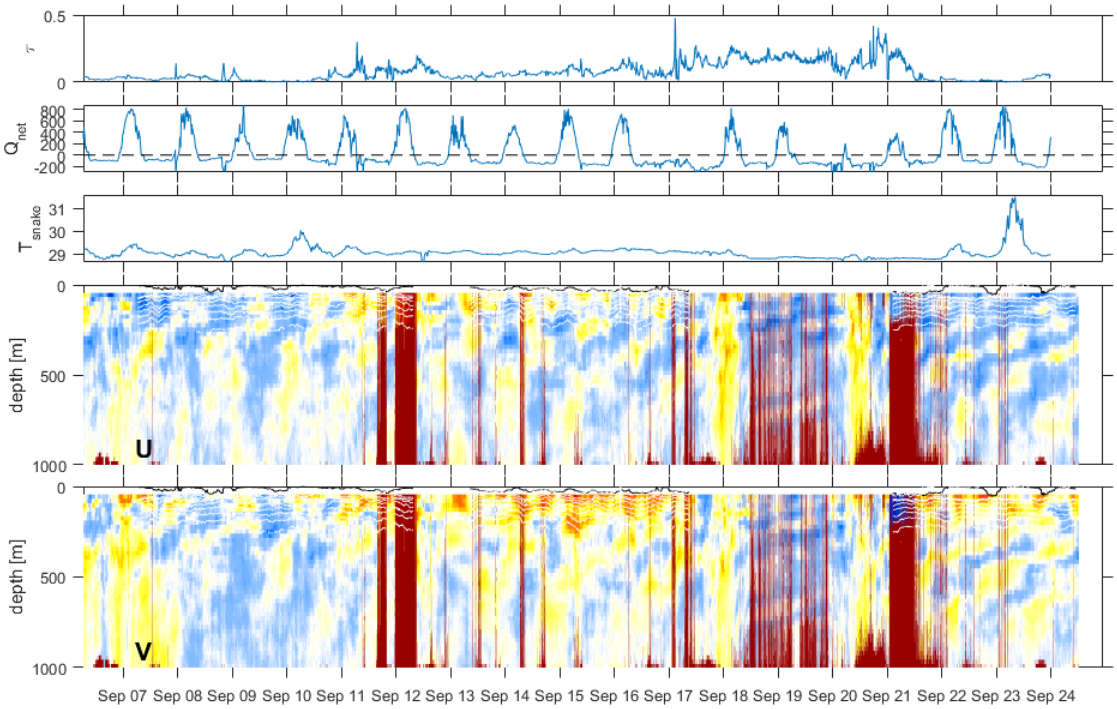

Figure 7 Wind stress, net surface heat flux, SST, u,v currents (OS38 kHz). Bubble contamination of the signal during heavy seas is indicated by dark red.

Two case studies from Chameleon ops during PISTON19

The middle part (mid-September) of PISTON19 was characterized by strong winds and rough seas due to a storm alternately known as Invest 95W, then TD18, then Tropical Storm Tapah. During this time, strong mixing occurred throughout the mixed layer, the base of which was at approximately 60 m. Turbulence dissipation rates exceeded 10^-7 m2/s3 throughout much of the mixed layer.

Starting around the 21st of September, the remnants of the storm left the operating region, and were replaced with the calmest winds we observed during the whole trip. A two-day record of the wind speed and the associated turbulence dissipation is shown.

Without the strong wind forcing, the turbulence decays over many hours due to the formation of diurnal warm layers on the 22nd and 23rd of September. Increased dissipation occurs during convective cooling at nighttime, but without the wind forcing, this is much weaker than the previous nights.

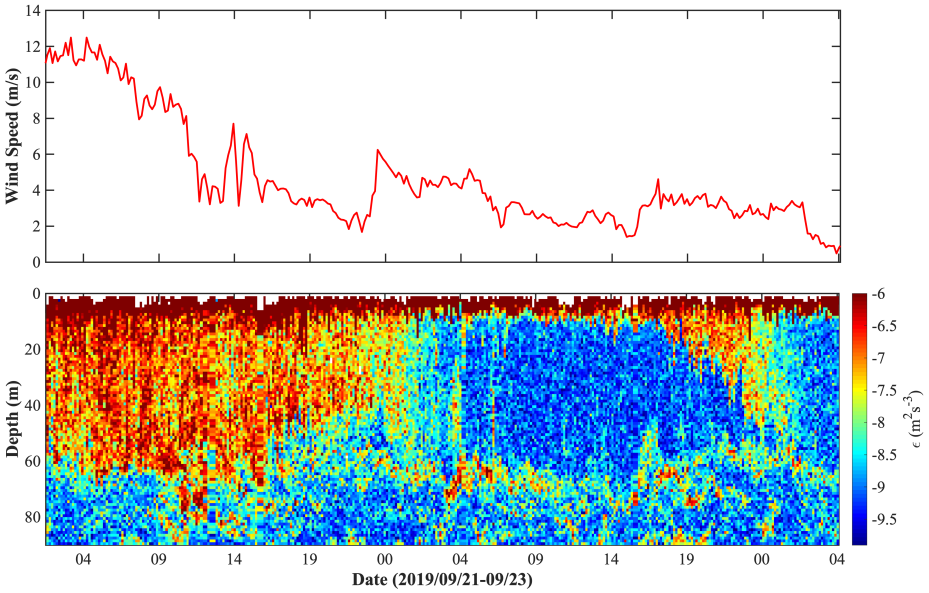

Figure 8 - A two-day record of turbulence measured by Chameleon clearly demonstrates the influence of wind on the mixing within the upper ocean.

Turbulence beneath the mixed layer, however, was strong several days after the winds decayed. Intense shear layers at 80 and 150 m depth are evident in the velocity records from the ship's 150 kHz ADCP. The structure of the velocity records suggests that the source of the shear is downward-propagating near-inertial waves, presumably due to the abrupt change in wind speed described above. Associated with the shear layers are layers of increased dissipation.

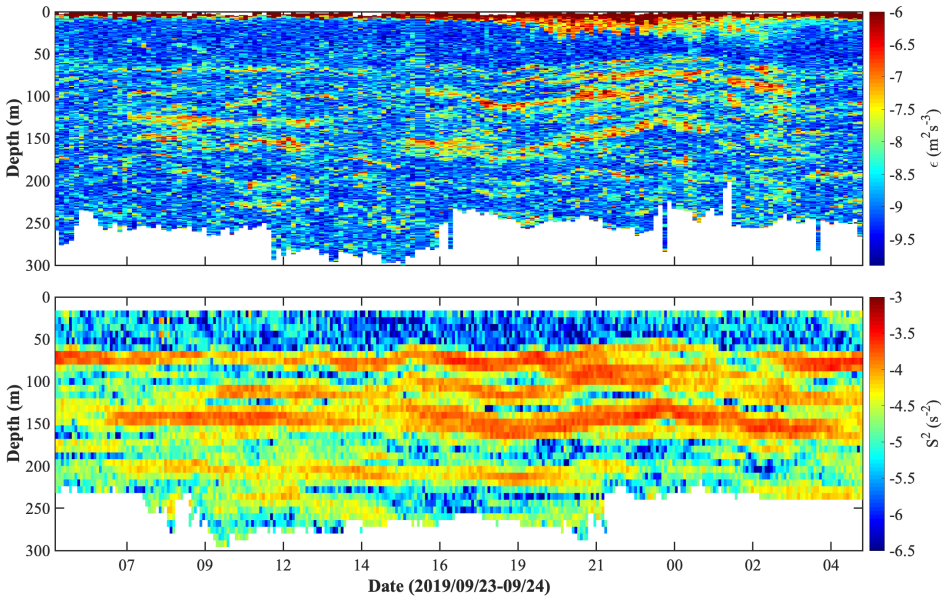

Figure 9 - Turbulent layers coinciding with layers of intense current shear observed from the ship's 150 kHz ADCP.